Sustainability of the Exploitation of Campi Flegrei Geothermal Area Using a Zero-mass Extraction Device

Claudio Alimonti (claudio.alimonti@uniroma1.it)

Sapienza University of Rome, DICMA, via Eudossiana 18 - 00184 Roma https://orcid.org/0000-0003-4113-9060

Elena Soldo

Sapienza University of Rome, DICMA, via Eudossiana 18 - 00184 Roma

Gennaro Sepede

Department of Applied Physics and Naval Technology, Universidad Politécnica de Cartagena (UPCT), Campus Alfonso XIII - 30203 Cartagena, claudio.alimonti@uniroma1.it, elena.soldo@uniroma1.it, gennaro.sepede@edu.upct.es, salvador.glopera@upct.es

Salvador Ángel Gómez-Lopera

Department of Applied Physics and Naval Technology, Universidad Politécnica de Cartagena (UPCT), Campus Alfonso XIII - 30203 Cartagena, claudio.alimonti@uniroma1.it, elena.soldo@uniroma1.it, gennaro.sepede@edu.upct.es, salvador.glopera@upct.es

Research

Keywords: geothermal energy, deep borehole heat exchanger, reservoir model, SHEMAT, CampiFlegrei

Posted Date: July 29th, 2020

DOI: https://doi.org/10.21203/rs.3.rs-49637/v1

Sustainability of the exploitation of Campi Flegrei geothermal area using a zero-mass extraction device

Claudio Alimonti[1], Elena Soldo[1], Gennaro Sepede[2] and Salvador Ángel Gómez-Lopera[2]

[1]Sapienza University of Rome, DICMA, via Eudossiana 18 - 00184 Roma

[2]Department of Applied Physics and Naval Technology, Universidad Politécnica de Cartagena (UPCT), Campus Alfonso XIII - 30203 Cartagena

claudio.alimonti@uniroma1.it

elena.soldo@uniroma1.it

gennaro.sepede@edu.upct.es

salvador.glopera@upct.es

Keywords: geothermal energy, deep borehole heat exchanger, reservoir model, SHEMAT, Campi Flegrei

Abstract

In this paper, the use of a zero-mass extraction device has been simulated in the volcanic area of Campi Flegrei (Italy), one of the most promising geothermal districts of Italy. The sustainability of the heat extraction has been studied with a coupled model of the geothermal reservoir and the deep borehole heat exchanger. The reservoir model has been built using the SHEMAT software, the heat transfer in the deep borehole heat exchanger has been simulated using GEOPIPE, a pure conductive semi-analytical model. An iterative approach has been used to couple the two simulators. The work has demonstrated that the area of Campi Flegrei is a promising candidate to produce sustainable geothermal energy with a zero-mass extraction device. It is also demonstrated that the coupled

model of reservoir and deep borehole heat exchanger is the best modelling approach when convective structures are present in the geothermal system, which can generate heat recovery effects.

Introduction

The area of Campi Flegrei is one of the most promising geothermal districts of Italy. The area is part of the Neapolitan volcanoes district, which includes also Ischia Island and Somma-Vesuvius volcano (Fig. 1).

Figure 1 – The Napolitan volcanoes district.

Campi Flegrei caldera is an active volcanic area famous for the thermal manifestations since Roman times, during which hot springs and fumaroles were used for thermal baths. Between 1930 and 1980 the main Italian energy companies and several scientific researchers carried out an exploration campaign on the Neapolitan volcanoes district, with the scope of understanding the geothermal potential of the area. More than 110 exploratory wells have been drilled to depths of 80-3046 m, demonstrating the presence of high-temperature fluids, even at relatively shallow depths. Nevertheless, the industrial exploitation has never taken off, because of the low price of oil in the '80s and the Italian energy strategy oriented on the nuclear sector. This one was abandoned after Chernobyl disaster in 1986 but, despite the growth of the environmental movement in the '90s, the interest on the exploitation of geothermal energy stored in Campi Flegrei area restarted only in recent times.

In 2010 the Legislative Decree n. 22 has promoted the development of new geothermal power plants in Italy, and two binary plants projects have been proposed in the Neapolitan geothermal area, respectively at Ischia island and Campi Flegrei. Furthermore, in 2012, a pilot well of 450 m deep was drilled in the eastern part of the Campi Flegrei caldera, within the Campi Flegrei Deep Drill Project

(CFDDP) in the framework of the International Continental Scientific Drilling Program (Carlino, 2018). The aim of the project was the improvement of the knowledge of physical properties of rocks hosting the reservoir and the collection of new data, necessary to model caldera dynamics. Anyway, the CFDD project has been stopped and none pilot plant has been realized in the area until today. The social response to the exploration and utilization of geothermal resources in the area of Campi Flegrei is negative. The caldera is one of the greatest geohazard areas on Earth (Piochi et al., 2014) and a great part of the population living there, perceive the drilling activities and the production and reinjection of fluids as an unacceptable risk.

The possibility to produce geothermal energy with a zero-mass extraction device may be the key to increase social acceptance. This solution entails the use of a deep borehole heat exchanger, or WellBore Heat eXchanger (WBHX), as named by Nalla et al. (2005). The heat exchanger is formed of an external steel casing and two internal coaxial tubes, also in steel (Fig.2). The internal tubes are separated by insulation, necessary to avoid heat exchange between the downward fluid and the upward one (Morita et al., 1992; Kohl et al., 2000; Kujawa et al., 2006; Wang et al., 2009). The coaxial heat exchanger acquires heat by conduction with the external ground and transfers the heat via conduction and convection to a working fluid which circulates in the device.

Figure 2: The coaxial heat exchanger.

The strength of this solution is that the mass extraction is avoided, preventing the cost and environmental risks related to the extraction, handling and reinjection of brine. Therefore, despite the low heat transfer effectiveness concerning the conventional geothermal wells, the coaxial heat exchanger could be an interesting opportunity for the exploitation of unconventional geothermal systems, like volcanic ones.

Despite the literature reports only 4 field tests of the deep borehole heat exchanger (Morita et al., 1992; Kohl et al., 2000 and 2002; Dijkshoorn et al., 2013), analysis of the performance of the WBHX are available. The authors have demonstrated that water is the most efficient heat carrier fluid and the most influencing parameter of heat extraction is the residence time (a function of the flow rate and the diameters) of the water in the exchanger (Alimonti and Soldo, 2016). The outlet temperature of the fluid is strongly affected by the geothermal gradient, the thermal conductivity and the volumetric heat capacity of the ground (Bu et al., 2012; Templeton et al., 2014). Concerning the productivity of the deep borehole heat exchanger, the value of 150 °C is the maximum wellhead temperature reported in the literature and the estimated thermal power is in the range 0.15–2.5 MW. The extracted heat could be converted in electricity using an Organic Rankine Cycle plant: the estimated values are in the range of 0.25–364 kW.

One of the main issues in pure conductive heat extraction devices is the reduction of power production in time. This phenomenon is due to the thermal disturbance and to the progressive enlargement of the thermal influence radius, which is in the range 20–50 m according to the evaluations of Kohl et al. (2002), Bu et al. (2012), Cei et al. (2013). Alimonti and Soldo (2016) demonstrated that after 1 year of continuous operation of the DBHE, the power production is 45% of the initial value. Mottaghy and Dijkshoorn (2012) demonstrated the sustainability of the use of a WBHX for heating purpose, thus operating with cycles of extraction and recovery.

The results of Mottaghy and Dijkshoorn (2012) also indicate that the presence of a groundwater flow has a positive effect on the deep borehole heat exchanger performance. The common approach to studying the heat extraction with a ground heat exchanger is the use of pure conductive models, whereas the evaluation of the groundwater influence on a coaxial heat exchanger, needs the simulation of the heat transfer into the reservoir and between it and the DBHE. In this case, the most accurate method entails the application of the conservation equation of mass, momentum and

92 energy in the heat exchanger and the surrounding rock, by using Multiphysics software, or coupling
93 a numerical reservoir model (i.e. TOUGH2, SHEMAT, FEFLOW) with a DBHE model (analytical,
94 semi-analytical, or numerical). Mottaghy and Dijkshoorn (2012) have highlighted that the great
95 computational time required by that software, can be drastically reduced, without losing accuracy,
96 coupling the reservoir model with a semi-analytical finite difference formulation for the WBHX.
97 In this paper, we simulate the use of a zero-mass extraction device in the volcanic area of Campi
98 Flegrei (Italy) using a coupled model of the geothermal reservoir and the deep borehole heat
99 exchanger. The reservoir model has been built using the SHEMAT software (Clauser, 2003), which
100 can simulate the brine production through wells, but not the production of heat via the WBHX. The
101 heat transfer in the deep borehole heat exchanger has been simulated using GEOPIPE (Alimonti and
102 Soldo, 2016), a pure conductive semi-analytical approach based on thermal resistances and the
103 Fourier equation. An iterative approach has been used to couple the two simulators. Then, the
104 simulation has been carried out using only the pure conductive semi-analytical model.
105 The paper has two main targets: to understand if the pure conductive simulation is a too
106 precautionary condition in presence of high temperature convective structures in the ground and to
107 study the sustainability of heat production via a zero-mass extraction device in the area of Campi
108 Flegrei. Two different operating modes have been evaluated: a constant flow rate scenario with the
109 maximum thermal power production and a constant thermal power scenario with a variable flow
110 rate. For the constant flow rate scenario, the coupling method uses the heat production values,
111 whereas for the constant thermal power scenario the temperature has been used to couple the two
112 simulators.

Campi Flegrei geothermal district

Figure 3 shows the Campi Flegrei geothermal district with his typical horse shape. The caldera located in the N-W limit of the Napoli gulf of Italy has a large diameter (12 km). The Figure reports some of the 26 wells drilled in the area.

Figure 3 - Campi Flegrei caldera.

The area of Mofete has been selected for the scope of this paper, having very high geothermal gradients (100–170 °C km^{-1}) resulting from the AGIP campaign (Fig. 4). The results indicate the presence of three main aquifers, of which the two shallower are the productive ones. The first aquifer is at the depth of 500-1000 m and has 20% in weight of non-condensable gases, the second one has a higher content of vapour (40%) and it is located between 1800 m and 2000 m (Fig. 4), the last aquifer is at the depth of 2500 with a thickness of 200 m. The total heat stored in the Mofete geothermal reservoir has been estimated around 1.08 × 1017 J by Carlino et al. (2012) using the method of Muffler and Cataldi (1978) and the recoverable energy is equal to 3.7 GW y.

Figure 4 – Temperature profiles with depth (Carlino et al. 2012).

This important quantity of heat is generated in the reservoir of Campi Flegrei, which contains a hot and saline geothermal system. According to Berrino et al. (1984) and Woo and Kilburn (2010), there is a relatively shallow magma sill at the depth lower than 3–4 km, whereas at the depth of 8–10 km is located the greatest magmatic source (Fig. 5), with a thickness of ~1 km and a diameter equal to that of the caldera (Zollo, 2008). The heat transfer in Campi Flegrei reservoir depends on the permeability: in the first kilometre the fracturing system produces a high hydrothermal circulation, so the advection is the main type of heat transport; between 1000 and 1800 the heat moves driven by

conduction; the presence of a second aquifer (1800–2000 m) guarantees the circulation of the fluids and so the advective mechanism; finally, at the depth greater than 3–4 km, the conduction is the heat transfer mechanism because the fluids circulate very slow (Carlino et al., 2016). The contribution of fluid advection is fundamental to simulate the actual thermal state of the shallow crust (Carlino et al., 2018). The simulation of the hydrothermal system has demonstrated that the bradyseism of Campi Flegrei area can be explained by hot fluid injection at the depth ≥ 3 km (Chiodini et al., 2003 and 2012; Troiano et al., 2011; Petrillo, 2013).

Figure 5 – Sketch of the geothermal system under the Neapolitan volcanoes district.

Methods

In this section, the simulation methods are presented.

The first model is GEOPIPE (Alimonti and Soldo, 2016), a purely conductive model of the heat transfer mechanisms in the zero-mass extraction device and between it and the ground. GEOPIPE is a semi-analytical approach able to estimate the ground thermal resistance in time, but not to simulate the natural hot fluid circulation and the possible thermal recovery. Therefore, the pure conductive method, fast and accurate for shallow probes, maybe a too precautionary approach for DBHEs when a high-temperature convective structure is present in the ground.

The authors have selected the SHEMAT software (Clauser, 2003) for the numerical simulation of the geothermal reservoir. The acronym SHEMAT means Simulator for HEat and MAss Transport, it is a general-purpose reactive transport simulation code. The selection of this simulator is explained by the necessity of an easy-to-use tool, adapt for a wide variety of thermal and hydrogeological problems. Nevertheless, the commercial version of SHEMAT does not include the DBHE simulation

159 tools, so the solution identified to simulate the interaction between the geothermal system and the
160 DBHE is the coupling of SHEMAT and GEOPIPE.

161 ## The semi-analytical model of BHE

162 The GEOPIPE simulator is a semi-analytical model based on thermal resistances (see Fig. 6). The
163 heat transfer into the ground source is modelled using an analytical solution of the Fourier equation
164 for heat transport. The evaluation of the actual thermal radius generated by the heat extraction,
165 $2\sqrt{\delta_s t}$, where δ_s is the thermal diffusivity of the formation and t is time, influences the thermal
166 resistance of the soil between the external well casing and the undisturbed ground (R_s) which is
167 calculated as:

168 $$R_s = \frac{1}{2\pi\lambda_s}\ln\left(\frac{2\sqrt{\delta_s t}}{r_{o,1}}\right) \qquad (1)$$

169 With λ_s the thermal conductivity of the solid and $r_{o,1}$ the external radius of the DBHE. The thermal
170 resistance model is composed of two terms: the thermal resistance between the downward fluid and
171 the undisturbed ground temperature, R_a, and the thermal resistance between the downward fluid
172 and the upward fluid R_b. As can be seen in Figure 6, R_a contains the conductive thermal resistance
173 of the soil R_s, the conductive thermal resistance between the two walls of the external casing (1 in
174 Fig. 7) and the convective thermal resistance between the downward fluid and the internal diameter
175 of the casing 1. R_d accounts for the convective thermal resistance between the downward fluid and
176 the external diameter of the casing 2, the conductive thermal resistance of the stratum composed by
177 the internal pipes and the insulator (3, 4, 5 in Fig. 7), the convective thermal resistance between the
178 upward fluid and the internal diameter of the tubing (5).
179 The convective coefficients of water ($k_{w,dw}$ and $k_{w,uw}$) have been calculated using the classical
180 Dittus-Boelter equation, adopting the same convection coefficient on the outer and inner surface due

181 to the full turbulence of the flow. The hydraulic diameter has been used for the calculation of Nusselt
182 and Reynolds numbers.

Figure 6 - Thermal resistances of the deep borehole heat exchanger.

Figure 7 – Deep borehole heat exchanger: axial view and materials.

183 The energy balance of the deep borehole heat exchanger is expressed by the following relation:

184 $$\dot{Q} = \dot{m}_w c_w \left(T_{w,uw} - T_{w,dw}\right) \qquad (2)$$

185 where, $\dot{Q}$ is the total heat exchanged by the working fluid with the ground.

186 The following set of differential equations is numerically solved finding the outlet temperature
187 which respects the condition $T_{out} = T_{w,uw}(0)$:

188 $$\begin{cases} \dot{m}_w c_w \dfrac{dT_{w,dw}}{dz}(z) = \dfrac{T_s(z) - T_{w,dw}(z)}{R_a} - \dfrac{T_{w,dw}(z) - T_{w,uw}(z)}{R_b} \\ -\dot{m}_w c_w \dfrac{dT_{w,uw}}{dz}(z) = \dfrac{T_{w,dw}(z) - T_{w,uw}(z)}{R_b} \end{cases} \qquad (3)$$

189 The mass flow rate, $\dot{m}_w$, and the inlet temperature are defined as input conditions, whereas the
190 imposed boundary conditions are:

191 $$T_{w,dw}(L = 0) = T_{in} \quad T_{w,dw}(L) = T_{w,up}(L) \qquad (4)$$

192 To run the GEOPIPE simulation, the input file must be compiled with the diameters composing the
193 DBHE (Tab. 1), the thermal conductivity of materials composing the DBHE (Tab. 2), the selected
194 working fluid, the inlet temperature, inlet pressure and flow rate of the working fluid (Tab. 3) and
195 the thermophysical properties of the soil (Tab. 4).

196 According to the results reported in the literature and illustrated in the background section, the
197 selected working fluid is water. Input temperature of 40 °C has been used, to evaluate a thermal use
198 of the resource. The flow rate imposed in scenario A is 20 $m^3\,h^{-1}$ (5.5 $kg\,s^{-1}$), which assures the

maximum thermal power production in time. The second scenario proposes a variable flow rate to produce a constant thermal power of 3 MW.

The model of the surrounding rock is composed by 5 different layers; the thermo-physical properties (Tab. 4) are taken by the contributes of Carlino et al. (2016), Troise et al. (2001), Troiano et al. (2011), Petrillo et al. (2013). A value of 35 °C has been assumed for the ground temperature at z_0. Considering the high temperatures of the ground in contact with the deep borehole heat exchangers, the only casing material considered in literature is steel. The proposed insulator material for this evaluation is air.

Regarding the calculation of the ground temperature with depth, GEOPIPE can operate in two modes: the operator can assign a geothermal gradient and the ground temperature at z_0, so the simulator produces the temperature profile; the operator assigns the temperature profile directly. This second option is that one followed for our analysis.

The reservoir mathematical model

Modelling the real geothermal reservoirs is a complex multidisciplinary problem that links physical and mathematical problems in which multiple approximations and unknowns are introduced. The results and solutions must be congruent and comparable with the measurements of the thermal and hydro-geological characteristics of the reservoir.

The first theoretical study of the geothermal problem was developed in the last century and it was derived from the fluid dynamic problem. An example is the Rayleigh (1916) dimensionless study or recently the one of Cánovas et al. (2017), having the aim of investigating the influence of the characteristics of porous media on the response of the domain.

Firstly, the main difficulty in studying the response of geothermal systems is to solve complex differential equation systems including the well-known conservation of momentum (or mass) and

222 energy equations in the form of different laws, e.g., Fourier or Darcy laws. The second issue is related
223 to the simplifications applied to the solid matrix of the soil and the fluid in the pores. For example,
224 the numerous approximations on the fluid dynamics for obtain different a models.
225 In the case of Campi Fregrei reservoir, many approximations are performed to solve the numerical
226 problem and define the response of the domain. One of these approximations is related to the
227 distribution of the thermo-fluid dynamic characteristics in the domain. Although considered as a
228 multi-layer, the studied domain is fully-heterogeneous which results in an anisotropic distribution
229 of the dynamic characteristics in the three spatial directions. Furthermore, some of them have
230 variable behaviours with temperature and pressure. These approximations, if not controlled
231 carefully, can vary significantly the solution obtained.
232 Typically, the fluid dynamic response of the system is studied through various coupling system of
233 equations such as a function of the velocity vector, the equipotential flow curves or the piezometric
234 height.
235 The continuity equation or equation of conservation of mass (Bejan and Kraus 2003; Clauser 2003;
236 Rühaak et al., 2008; Luo et al., 2015; Liu et al., 2020) for the groundwater unsteady flow in a saturated
237 anisotropic confined aquifer (the porous medium), without fluid sources or sinks and in the
238 assumption of the medium can be compressed, both the solid matrix (skeleton) and the fluid, can be
239 written in the form

240 $$\frac{\partial(\varphi\rho_f)}{\partial t} + \nabla\cdot\left(\rho_f\vec{v}\right) = 0 \quad (1)$$

241 where $\vec{v}$ is the Darcy velocity

244 $$\vec{v} = \frac{\tilde{k}}{\mu}\left[-\nabla P + \rho_f\vec{g}\right] \quad (2)$$

242 $\tilde{k}$ is the anisotropic hydraulic permeability diagonal tensor, with components k_x, k_y and k_z along
243 each of the three spatial directions. Defining the hydraulic constant density reference potential

(head) h, the fluid relative density ρ_r respect to a reference state with density ρ_0 and the hydraulic conductivity tensor $\widetilde{K}$ for the anisotropic porous medium as

$$h = z + \frac{P}{\rho_0 g} \qquad \rho_r = \frac{\rho_f - \rho_0}{\rho_0} \qquad \widetilde{K} = \frac{\rho_f g \tilde{k}}{\mu} \qquad (3)$$

it is immediate to relate time derivative and gradient of P with the corresponding for h. Then, after several calculations, it is possible to express equation (1) in terms of piezometric height or reference potential h

$$S_s \frac{\partial h}{\partial t} - \frac{\partial}{\partial x}\left(K_x \frac{\partial \mathrm{h}}{\partial x}\right) - \frac{\partial}{\partial y}\left(K_y \frac{\partial h}{\partial y}\right) - \frac{\partial}{\partial z}\left(K_z \left(\frac{\partial h}{\partial z} + \rho_r\right)\right) = 0 \qquad (4)$$

The specific storage coefficient S_s (m^{-1}) is defined from solid (α) and fluid (β) isothermal compressibility as a linear model (Cooper, 1966; Galloway and Burbey, 2011; Kuang et al., 2020) in the form $S_s = \rho_f g(\alpha + \phi\beta)$. For the skeleton, that is, the solid part of the porous medium (rock), compressibility was fixed with a constant value $\alpha = 1.00\times10^{-10}$ Pa^{-1}. Compressibility $\beta(T, P)$ of the fluid part (pore fluid) was updated internally by SHEMAT at each time step using the varying temperature and pressure values.

For establishing the energy conservation equation in the porous medium, assuming the thermodynamic equilibrium between groundwater and soil is instantaneous, then both fluid and soil have the same temperature (Luo et al., 2015). Considering a finite volume of the medium, including the fluid and solid part, a conductive-convective physical model can be written for an anisotropic matrix in three directions in term of temperature and fluid velocity (Clauser, 2003; Bejan and Kraus, 2003, Rühaak et al., 2007). Let $Q = \rho c T$ be the heat of a control volume in the porous medium, where ρc is the volumetric thermal capacity of the medium. Then, the heat rate $\dot{Q} = \frac{\partial Q}{\partial t}$ will be $\frac{\partial}{\partial t}(\rho c T)$ and, if there is no heat sources present in the volume and the viscous energy dissipation and the thermal compressibility effects of the fluid are negligible, the convection-diffusion equation

for the heat transport in the control volume of the porous medium can be written as (Clauser, 2003; Bejan and Kraus, 2003; Liu et al., 2020)

$$\frac{\partial}{\partial t}(\rho c T) = \nabla \cdot \left(\tilde{\lambda} \nabla T\right) - \rho_f c_f \vec{v} \cdot \nabla T \qquad (5)$$

where $\tilde{\lambda}$ (W m^{-1} K^{-1}) is the bulk thermal conductivity tensor or effective conductivity diagonal tensor, with components, for an anisotropic medium, λ_x, λ_y, λ_z along each of the three spatial directions. Both, ρc and $\tilde{\lambda}$, are defined for the porous medium as average properties in order to consider the solid matrix (rocks) and the fluid in the pores like a weighted arithmetic mean, in the form

$$\rho c = \rho_f c_f \varphi + (1 - \varphi)\rho_s c_s \qquad (6)$$

$$\tilde{\lambda}(\varphi, T, P) = \varphi \tilde{\lambda}_f(T, P) + (1 - \varphi)\tilde{\lambda}_s(T) \qquad (7)$$

Equation (6) implies that during a differential time interval dt, porosity and the other material properties are constant. Then, equation (5), in extended form, is

$$\rho c \frac{\partial T}{\partial t} - \frac{\partial}{\partial x}\left(\lambda_x \frac{\partial T}{\partial x}\right) - \frac{\partial}{\partial y}\left(\lambda_y \frac{\partial T}{\partial y}\right) - \frac{\partial}{\partial z}\left(\lambda_z \frac{\partial T}{\partial z}\right) + \rho_f c_f \left(\frac{\partial T}{\partial x} v_x + \frac{\partial T}{\partial y} v_y + \frac{\partial T}{\partial z} v_z\right) = 0 \qquad (8)$$

The reservoir mathematical model is constituted for the equations (4) and (8), a system of two partial differential equations in the unknows h and T, simply substituting equations (2 and 3) into equation (8). Boundary and initial conditions, presented next, complete the model for defining the geothermal problem of Campi Flegrei presented in this work.

DBHE properties and thermo-physical parameters. Spatial discretization. Boundary andinitial conditions

Diameters composing the DBHE, thermal conductivity of DBHE materials and working fluid input values in DBHE are presented in the next tables.

Table 1 – Deep borehole heat exchanger diameters.

1	9 ⅝ inch	OD 244.4 mm	ID 226.6 mm

3	7 inch	OD 177.80 mm	ID 150.36 mm
5	3 ½ inch	OD 88.90 mm	ID 77.92 mm

288

Table 2 - Thermal conductivity of DBHE materials.

Material	Thermal conductivity ($W\ m^{-1}\ K^{-1}$)
Air	0.026
Steel	50

Table 3 – Working fluid input values in DBHE.

Working fluid	Water
Inlet temperature	40 °C
Inlet pressure	25 Bar
Flow rate A	20 $m^3\ h^{-1}$
Flow rate B	variable

289

290 The thermo-physical parameters of Campi Flegrei obtained from the studies of Carlino (2018),
291 Carlino et al. (2016) and Troise et al. (2001) allow the identification of six homogenous isotropic
292 layers which describe the behaviour of the reservoir (Tab. 4).

293 **Table 4: Thermo-physical properties of the soil.**

Zone (Layer)	Zone Thickness (m)	Porosity	Geothermal gradient (for DBHE) (10^{-2} °C m^{-1})	Permeability (m^2)	Thermal conductivity ($W\ m^{-1}\ K^{-1}$)	Density ($kg\ m^{-3}$)	Specific Heat ($J\ kg^{-1}K^{-1}$)
1	0-500	0.3	15.0	10^{-15}	2.1	1800	1000
2	500-1000 (aquifer)	0.3	15.0	10^{-14}	2.1	2100	1000
3	1000-1400	0.3	15.0	10^{-18}	2.1	2400	1000
4	1400-1800	0.3	15.0	10^{-17}	2.1	2400	1000

5	1800-2000 (aquifer)	0.3	15.0	10^{-15}	2.1	2400	1000
6	2000-3000	0.3	No DBHE	10^{-18}	2.1	2400	1000

294

295 To numerically solve the three-dimensional problem of Campi Fregrei, a regular domain with a
296 longitudinal size of 6000 m (as proposed in Troise et al., 2001), depth of 3000 m (as proposed in
297 Carlino et al., 2016; Petrillo et al., 2013; Troiano et al., 2011; Troise et al., 2001;) and three cross-
298 sections spaced 10 m along Y axis, have been built with SHEMAT software (Fig. 8). The domain is
299 discretized through a node-centred grid. The hypothesis of a borehole in the centre of the model has
300 been used. Therefore, the grid cell sizes are $\Delta x\Delta y\Delta z = 50\times10\times50$ m^3 and a refinement has been done
301 for the 5 central cells in the position of the DBHE ($\Delta x\Delta y\Delta z = 10\times10\times50$ m^3). Table 5 shows the grid
302 composition.

Table 1 – Grid of Campi Flegrei domain.

Plain	Rows	Columns
X-Z	60	124
X-Y	3	124
Z-Y	60	3

Figure 8 – Campi Flegrei domain.

303 Due to the complexity of the geothermal field and the coupling with the WBHX, severe boundary
304 conditions have been implemented (see Fig. 9). The flow boundary conditions specify the mass flux
305 from the lateral borders (as in Troise, 2011) and at the bottom of the domain (as in Troiano et al. 2011
306 and Petrillo et al., 2013). The initial constant value of the lateral flux is 7×10^{-11} m s^{-1}; the flux at the
307 bottom is distributed orthogonally through the discretized elements, with two different values,
308 8×10^{-10} m s^{-1} in the central part and 4×10^{-11} m s^{-1} for rest of the bottom cells. The hydrostatic load is
309 set equal to the domain elevation i.e. 3000 m.

Using the contributes of Carlino (2018), Carlino et al. (2016), Troiano et al. (2011) and Troise et al. (2001), a specific constant thermal source has been defined as a boundary condition for temperature. Besides, an increasing temperature gradient with a maximum value of 400 °C in the central part is defined at the bottom of the domain. The temperature at the top of the reservoir has a temporally constant value of 35 °C. Considering the position of the magmatic heat source of the domain, which is sufficiently distant from the vertical walls, an adiabatic thermal condition can be assumed at the lateral walls as in Petrillo et al. (2013). The initial temperature in the whole domain is zero.

Initial and boundary conditions and the layer discretization are illustrated in the next figure. Once the initial and boundary conditions are applied, the system is discretized in its transient state using the finite difference method with a central difference resolution scheme (Il'in, 1969).

Figure 9 - Boundary conditions imposed in SHEMAT model of Campi Flegrei.

The coupling of DBHE model and reservoir model

The target of the coupling of GEOPIPE simulator with SHEMAT software is to create a tool that simulates the heat transfer in the reservoir, in the deep borehole heat exchanger and between them. The first step has been the modification of GEOPIPE code to remove the calculation of the ground thermal radius in time, which is simulated by SHEMAT software. The flowcharts in Fig. 10 explain the two process of coupling GEOPIPE and SHEMAT: the ground temperature, $T(z,t)$, the heat production via WBHX, $H(z)$, and the fluid temperature in the annulus, $T_{w,dw}$, are the parameters required for the coupling. The SHEMAT software runs and produces a temperature pattern in every cell of the domain for the initial time t_0. The ground temperature values at the interface of the DBHE are used as input in GEOPIPE simulator. In method A (Fig. 10 (a)) GEOPIPE runs and estimates the heat acquired, $H(z,t^*)$, from the surrounding ground after each selected time step. The heat production required by SHEMAT, (HPROD), is the heat referred to the cell volume, that is the

ground cell in contact with the borehole wall. The $H(z, t^*)$ values are copied in the input file of SHEMAT and another run simulates the thermal influence generated on the ground after time t^*. The procedure is repeated changing the simulation time (t^*) in SHEMAT.

Figure 10 (a) – Method A

Figure 10 (b) – Method B

Figure 10: Workflow of the two models coupling.

Method B (Fig. 10 (b)) uses a constant thermal power scenario which is more realistic by the operative point of view. The produced power is fixed and the WBHX flow rate is changed during the lifetime of the plant, depending by the ground temperature extracted by SHEMAT simulator. The values of temperature $T_{w,dw}$ are used as input WBHX temperature in SHEMAT. This temperature is lower than the medium temperature of the fluid in the DBHE at the generic depth z, which is usually used in the studies regarding the geothermal probes. Anyway, the authors consider that the values of temperature of the ground in contact with the borehole walls are very near to the temperature of the fluid in the annulus and an eventual deviation from the real values is a precautionary underestimation.

Results and discussion

The first target of this study has been the replication of the temperature pattern of Campi Flegrei, to apply a zero-mass extraction device in a reservoir model, as much as possible similar, to the literature and surveys data. The results reported in Figure 11 confirms the accuracy of the model: the temperature curves indicate the presence of the small magma sill at a depth lower than 3–4 km and the propagation towards the surface of the thermal perturbation.

Figure 11 – Initial temperature pattern.

355 The temperature is very high at the bottom, about 400 °C at the depth of 2850 m. Figure 11 depicts
356 the steady-state condition, before the deep borehole heat exchanger starts to operate, both for the
357 constant flow rate scenario and the constant thermal power scenario.

358 **Scenario A: constant flow rate**

359 In this section, the results of the simulations of continuous operation of a DBHE with a flow rate of
360 20 $m^3 h^{-1}$ are presented. The Figures 12-14 illustrates the results obtained with the coupled
361 SHEMAT-GEOPIPE model, whereas the comparison of the results obtained with the two
362 approaches is reported in Figures 15 and 16.
363 Figure 12 shows that the heat production decreases in time and the higher values of heat production
364 are in correspondence of the shallow aquifer (500–1000 m). Since 3 months, the curves present an
365 anomalous trend which can be explained with an instability of the solution. This phenomenon could
366 indicate that the proposed procedure guarantees the precision of the results until the time step is
367 limited (about 30 days).
368 Figure 13 shows the thermal disturbance induced on the ground surrounding the deep borehole
369 heat exchanger. The curves are referred to as the first column in contact with the borehole wall. The
370 data highlight that the decrease in temperature is limited in the first days but reaches 40 °C after 1
371 month of operation. Then, the continuous heat extraction with a $m^3 h^{-1}$ flow rate induces a
372 maximum decrease of 200 °C in 3 years, demonstrating that the selected operation conditions are not
373 sustainable in time.
374 Figure 14 illustrates the progressive enlargement of the thermal disturbance in time. The influence
375 radius after 1 month of operation (Fig. 14 (a)) is about 10 m, it reaches 25 m after 6 months and it
376 remains stable since 1 year (Fig. 14 (b) and (c)). The thermal radius reaches 50 m after 3 years of heat
377 extraction with a DBHE (Fig. 14 (d)). The discussed results show a massive temperature decrease
378 and a considerable thermal interference that seem inconsistent with the use of deep borehole heat

exchangers. The authors consider that the reason for these results could be explained with the use of too high values of heat production. It is unclear what volume is used for the evaluation of heat production (expressed in W m^{-3}) in SHEMAT software.

Figure 12 - Heat extracted in time vs depth (SHEMAT – GEOPIPE model); fixed flow rate scenario.

Figure 13 - Decrease of the ground temperature in contact with the DBHE (SHEMAT – GEOPIPE model; fixed flow rate scenario.

Figure 14 (a) – 1-month simulation results.	**Figure 14 (b) – 6-month simulation results.**
Figure 14 (c) – 1-year simulation results.	**Figure 14 (d) – 3-year simulation results.**

Figure 14- Thermal disturbance variation; fixed flow rate scenario.

The histograms in Figures 15 and 16 show the comparison of the results obtained with the two approaches demonstrating that the pure conductive model (GEOPIPE) is more adequate than the conductive one (SHEMAT–GEOPIPE), because the second overestimates the production. GEOPIPE estimates a maximum produced temperature of about 147 °C, whereas the coupled model indicates a value greater to 250 C° that decreases after 3 months of operation. The producible thermal power evaluated with SHEMAT–GEOPIPE model is greater than 6.5 MW for the first month, then decreasing to about 2 MW at 5 years of operation. The values estimated with GEOPIPE are much lower, with values of 2.3 MW after 1 day of operation that decreases to 867 kW at 5 years.

Figure 15 - Decrease of water temperature extracted by a zero-mass extraction device; fixed flow rate scenario.

Figure 16 - Sustainability in time of a zero-mass extraction plant; fixed flow rate scenario.

The graph in Figure 17 indicates that the pure conductive approach produced a steady-state condition of the thermal decline after 3 months. Otherwise, a recovery action of the outlet temperature is estimated with SHEMAT–GEOPIPE model for 5 years of operation. This phenomenon could indicate that the proposed model can replicate the effect of the high-temperature convective structures in the ground. Anyway, the severe decline of the temperature in the cells in contact with the borehole walls, makes impossible to proceed with the simulation.

Figure 17 – Thermal decline in time; fixed flow rate scenario.

Scenario B: constant thermal power

Starting from the results discussed in the previous section, a constant thermal power scenario has been studied. For this scenario a refinement of the reservoir model has been carried out, using a base mesh grid size of 25×25 m^2 and further refinement in the surrounding of the well (1×25 m^2) until reaching the dimensions of 0.2×25 m^2 for the DBHE cells. The three cross-sections have been not changed.

Using the pure conductive GEOPIPE simulator, the maximum thermal power that can be sustained for 10 years of continuous operation has been investigated. The selected value of 850 kW requires a maximum flow rate of 27 $m^3\ h^{-1}$ after 10 years of operation (Fig. 18) when the produced temperature is strongly reduced to the value of 79 °C, which is still useful for various direct use applications.

Figure 18 – Variation of flow rate and outlet temperature for a DBHE operating at a fixed thermal power of 850 kW; Geopipe results.

The values of heat production per cubic meter (Fig. 19) along with depth highlight the presence of two zones, an insulating one between 50 m and 800 m and a conductive layer between 1000 m and 2000 m.

Figure 19 – Heat production along with depth at a fixed thermal power of 850 kW.

These two zones are characterized by different values of rock density (see Tab. 4) and so of thermal diffusivity, which affects the temperature gradient between the ground and the fluid in the annulus. As can be seen in Fig. 19 the heat production curve is the reflecting curve of the temperature difference curve. The strong numerical difference of heat production values respect to those of the constant flow rate scenario is explained by the refinement of the mesh: this paradox highlights the complexity of defining the right volume to refer the heat production for SHEMAT input file.

Figure 20 illustrates the thermal disturbance induced on the first column in contact with the borehole wall, using the coupled model SHEMAT-GEOPIPE. The data highlight that the decrease in temperature is very low, with maximum values of 2 °C in the first 1000 m of depth, after 5 days and 1 month of operation. On the other hand, between 1000 and 2000 m of depth, there is an increase of 2 °C after 2 days, 1 month and 3 months of operation. Generally, as can be seen, when the operation period increases, the temperature is more stable, probably due to the recharge effect generated by the convective structures of the reservoir. The results indicate that the heat extraction with a WBHX operating at a fixed thermal power of 850 kW does not affect the thermal field of Campi Flegrei reservoir, so the plant is sustainable in a long time.

Figure 20 - Decrease of the ground temperature in contact with the DBHE (SHEMAT – GEOPIPE model; fixed thermal power scenario.

444 The histogram in Figure 21 and the thermal decline shown in Figure 22 confirm the sustainability of
445 the WBHX and the too precautionary approach of the pure conductive analytical model, in presence
446 of a thermal source and advective mechanisms in the geothermal system. The outlet temperature of
447 the fluid circulating in the deep borehole heat exchanger remains very high (309 °C) with the coupled
448 model, while the pure conductive method estimates a decrease of 131.5 °C and 213.6 °C of
449 temperature, after 1 year and 10 years of operation respectively.
450
451 **Figure 21 – Decrease of water temperature extracted by a zero-mass extraction device; fixed thermal power scenario.**
452
453 **Figure 22 – Thermal decline in time; fixed thermal power scenario.**

454 ## Conclusions

455 The present work evaluates the production of geothermal energy with a zero-mass extraction device
456 applied in the volcanic area of Campi Flegrei, Italy. The area is characterized by very high thermal
457 gradients, but this potential is underused, and the geothermal sector meets social resistances.
458 Therefore, the possibility to produce geothermal energy, avoiding all the risks related to the brine
459 extraction, seems to be very interesting in this area.
460 The paper is focused on the identification of the most correct simulation method to study the thermal
461 influence of the heat extraction device on the geothermal reservoir with convective structures, as in
462 the case of Campi Flegrei. Two methods have been compared: a pure conductive semi-analytical
463 model, and a coupled model composed by of numerical model for the reservoir and an analytical
464 model for the DBHE. The first approach, fast and accurate for shallow probes, is not able to simulate
465 the natural hot fluid injection from the bottom and the possible thermal recovery, which guarantees
466 the sustainability of the heat extraction.

Two different operating modes have been evaluated for the coupled model: a constant flow rate scenario of 20 $m^3\ h^{-1}$, which assures the maximum thermal power for the selected design, using the heat production values to couple the reservoir model and the DBHE model; a constant thermal power scenario of 850 kW, using the temperature of the fluid in the device to couple the two models. The results have shown very impressive temperature decrease in the ground surrounding the WBHX when it operates with a fixed flow rate of 20 $m^3\ h^{-1}$, with a decrease of 200 °C in 3 years. The influence radius after 1 month of operation is about 10 m and it reaches 50 m after 3 years. These results indicate that the selected heat production values are not sustainable in time and have revealed the uncertainty of the coupling using heat production.

The second scenario estimates a negligible decrease of temperature, with maximum values of 2 °C. The results indicate that the heat extraction with a WBHX operating at a fixed thermal power of 850 kW does not affect the thermal field of Campi Flegrei reservoir, probably due to the recharge effect generated by the convective structures of the reservoir, so the plant is sustainable in time.

The output of the pure conductive model is very different, not simulating any thermal source into the ground. The temperature of the produced fluid is decreased by 43 °C after 1 month of operation, and 213.6 °C in 10 years.

In conclusion, the work has demonstrated the feasibility of the use of a zero-mass extraction device in the area of Campi Flegrei to produce sustainable geothermal energy. It is also demonstrated that in case of geothermal systems in which the heat flows not only by conduction but also by convection, only the coupled model of reservoir and deep borehole heat exchanger can depict the exchanges between the DBHE and the thermal field and the effects on DBHE heat recovery.

Regarding the geothermal reservoir model, the results and the comparison with literature data, confirm the accuracy of the proposed model and the SHEMAT software. However, the available

commercial version of the software does not allow to implement the DBHEs and the authors had to provide an appropriate, even if not easy and quick, coupling method.

Declarations

Availability of data and materials

Data sharing is not applicable to this article as no datasets were generated or analysed during the current study.

Competing interests

The authors declare that they have no competing interests

Funding

The present work was undertaken without any funding

Authors' contributions

CA had contribute by modifying the software Geopipe used in the work; ES and GS designed the work, defined the modelling strategy and did the results analysis; SAGL has contributed to the revision of the work.

Acknowledgements

Not applicable

References

Alimonti, C., Soldo, E., Bocchetti, D., Berardi, D.: The wellbore heat exchangers: A technical review, Renewable Energy, 123, (2018), 353-381.

Alimonti, C., Soldo, E.: Study of geothermal power generation from a very deep oil well with a wellbore heat exchanger, Renewable Energy, 86, (2016), 292-301.

Bejan A, Kraus AD: Heat transfer handbook, Wiley-Interscience, Har/Cdr edition (2003), pp. 1138

512 Berrino, G., Camacho, A.G., 2008. 3D gravity inversion by growing bodies and shaping layers at Mt.
513 Vesuvius (southern Italy). Earth Sciences and Mathematics. Birkhäuser, Basel, pp. 1095–1115.
514 Bu, X., Ma, W., Li, H.: Geothermal energy production utilizing abandoned oil and gas wells,
515 Renewable Energy, 41, (2012), 80-85.
516 Cánovas, M., Alhama, I., García, G., Trigueros, E., Alhama F.: Numerical simulation of density-
517 driven flow and heat transport processes in porous media using the network method. Energies, 10
518 (9), (2017), art. no. 1359.
519 Carlino, S.: Heat flow and geothermal gradients of the Campania region (Southern Italy) and their
520 relationship to volcanism and tectonics, Journal of Volcanology and Geothermal Research, 365,
521 (2018) 23-37.
522 Carlino, S., Troiano, A., Di Giuseppe, M.G., Tramelli, A., Troise, C., Somma, R., De Natale, G.:
523 Exploitation of geothermal energy in active volcanic areas: A numerical modelling applied to the
524 high temperature Mofete geothermal field, at Campi Flegrei caldera (Southern Italy), Renewable
525 Energy, 87, (2016), 54-66.
526 Carlino, S., Somma, R., Troise, C., De Natale, G.: The geothermal exploration of Campanian
527 volcanoes: Historical review and future development, Renewable and Sustainable Energy Reviews,
528 16, (2012), 1004– 1030.
529 Chiodini, G., Todesco, M., Caliro, S., Del Gaudio, C., Macedonio, G., Russo, M.: Magma degassing
530 as a trigger of bradyseismic events: the case of Phlegrean Fields (Italy). Geophys. Res. Lett. 30 (8),
531 (2003), 1434–1437.
532 Chiodini, G., Caliro, S., DeMartino, P., Avino, R., Gherardi, F.: Early signals of new volcanic unrest
533 at Campi Flegrei caldera? Insights from geochemical data and physical simulations. Geology, 40,
534 (2012), 943–946. http://dx.doi.org/10.1130/G33251.1.

Clauser, C.: Numerical Simulation of Reactive Flow in Hot Aquifers: SHEMAT and Processing SHEMAT, Springer, Heidelberg-Berlin (2003).

Cooper, H.: The equation of Groundwater flow in fixed and deforming coordinates, Journal of Geographical Reserch, Vol. 71, No. 20, 1966.

Dijkshoorn L, Speer S and Pechnig R: Measurements and Design Calculations for a Deep Coaxial Borehole Heat Exchanger in Aachen, Germany. Hindawi Publishing Corporation International Journal of Geophysics, Volume 2013, Article ID 916541, 14 pages. http://dx.doi.org/10.1155/2013/916541.

Galloway, D., Burbey, T.: Rewiew: Regional land subsidence accompanying groundwater extraction, Hydrogeology Journal (2011) 19: 1459-1486, Springer-Verlag.

Kohl, T., Brenni, R., Eugster, W.: System performance of a deep borehole heat exchanger, Geothermics, 31, (2002), 687-708.

Kuanga, X., Jiaoc, J., Zhenga, C., Cherrye, J., Lia, H.: A review of specific storage in aquifers, Journal of Hydrology 581 (2020) 124383.

Kujawa T., Nowak W., Stache, A.A.: Utilization of existing deep geological wells for acquisitions of geothermal energy, Energy, 31, (2006), 650-664.

Il'in A. M.: Differencing scheme for a differential equation with a small parameter affecting the highest derivative. Mat. Zametki, 6:2 (1969), 237–248; Math. Notes, 6:2 (1969), 596–602.

Lavine, A.S., DeWitt, D.P., Bergman, T.L., Incropera, F.P., (2011), Fundamentals of Heat and Mass Transfer (7th ed.). Hoboken (NJ): John Wiley & Sons, Inc.

Liu, G., Wang, G., Zhao, Z., Ma, F.: A new well pattern of cluster-layout for deep geothermal reservoirs: Case study from the Dezhou geothermal field, China. Renewable Energy 155 (2020) 484-499.

Luo, Z., Wang, Y., Zhou, S., Wu, X.: Simulation and prediction of conditions for effective development of shallow geothermal energy. Applied Thermal Engineering, 91 (2015), 370-376.

Morita K., Bollmeier W.S., Mizogami H.: An experiment to prove the concept of the downhole coaxial heat exchanger (DCHE) in Hawaii. Transactions - Geothermal Resources Council, 16, 1992, 9-16.

Mottaghy, D., Dijkshoorn, L.: Implementing an effective finite difference formulation for borehole heat exchangers into a heat and mass transport code. Renewable Energy, 45, (2012) 59-71.

Muffler, P., Cataldi, R.: Methods for regional assessment of geothermal resources, Geothermics, 7, (1978), 53–89.

Nalla, G., Shook, G.M., Mines, G.L. and Bloomfield, K.K.: Parametric sensitivity study of operating and design variables in wellbore heat exchanger, Geothermics, 34, (2005), 330–346.

Petrillo Z., Chiodini, G., Mangiacapra, A., Caliroa, S., Capuanob, P., Russo, G., Cardellini, C., Avino, R.: Defining a 3D physical model for the hydrothermal circulation at Campi Flegrei caldera (Italy). Journal of Volcanology and Geothermal Research, 264, (2013), 172–182.

Piochi M., Kilburn C. R. J., Di Vito M. A., Mormone A., Tramelli A., Troise C., De Natale G.: The volcanic and geothermally active Campi Flegrei caldera: an integrated multidisciplinary image of its buried structure. Int J Earth Sci (Geol Rundsch) (2014) 103:401–421, DOI 10.1007/s00531-013-0972-7.

Rayleigh, R.: On the convective currents in a horizontal layer of fluid when the higher temperature is on the under side. Phil. Mag. 32 (1916) 529–546.

Templeton, J.D., Ghoreishi-Madiseh, S.A., Hassani, F., Al-Khawaja, M.J.: Abandoned petroleum wells as sustainable sources of geothermal. Energy, 70, (2014), 366–373.

580 Troiano, A., Di Giuseppe, M.G., Petrillo, Z., Troise, C., De Natale, G.: Ground deformation at
581 calderas driven by fluid injection: modelling unrest episodes at Campi Flegrei (Italy), Geophys. J.
582 Int., 187, (2011), 833-847, http://dx.doi.org/10.1111/j.1365-246X.2011.05149.x.
583 Troise, C., Castagnolo, D., Peluso, F., Gaeta, F.S., Mastrolorenzo, G., De Natale, G.: A 2D mechanical-
584 thermalfluid-dynamical model for geothermal systems at calderas: an application to Campi Flegrei,
585 Italy. Journal of Vulcanology and Geothermal Research, 109, (2001), 1-12.
586 Wang, Z., McClure, M.W., Horne, R.N.: A single-well EGS configuration using a thermosiphon,
587 Proceedings, 34-th Workshop on Geothermal Reservoir Engineering Stanford University 2009,
588 Stanford, California, February 9-11, 2009.
589 Woo, J.Y., Kilburn, C.R., 2010. Intrusion and deformation at Campi Flegrei, southern Italy: sills,
590 dikes, and regional extension. J. Geophys. Res. Solid Earth 115 (B12).
591 Zollo, A., Maercklin, N., Vassallo, M., Dello Iacono, D., Virieux, J. and Gasparini, P.: Seismic
592 reflections reveal a massive melt layer feeding Campi Flegrei caldera, Geophys.Res.Lett., 35,
593 (2008).L12306, DOI:10.1029/2008GL03424.

594 NOMENCLATURE

595	c	specific heat capacity	[J kg^{-1} K^{-1}]
596	D_h	hydraulic diameter	[m]
597	g	gravitational acceleration	[m s^{-2}]
598	h	hydraulic potential, head	[m]
599	H	heat production via WBHX	[W m^{-3}]
600	k_w	convective heat transfer of water	[W m^{-2} K]
601	$\tilde{k}$	hydraulic permeability tensor	[m^2]
602	$\tilde{K}$	hydraulic conductivity tensor	[m s^{-1}]
603	L	total length of the well	[m]

$\dot{m}$	mass flow rate	$[\mathrm{kg\,s^{-1}}]$	
P	pressure	[Pa]	
$\dot{Q}$	total thermal power	[W]	
R	thermal resistance	$[\mathrm{mK\,W^{-1}}]$	
r	radius	[mm]	
T	temperature	[K or °C]	
t	time	[s]	
v	velocity	$[\mathrm{m^{-1}s^{-1}}]$	
z, Z	depth	[m]	

Greek symbols

α	solid (rock) compressibility	$[\mathrm{Pa^{-1}}]$	
β	fluid compressibility	$[\mathrm{Pa^{-1}}]$	
λ	thermal conductivity	$[\mathrm{W\,m^{-1}K^{-1}}]$	
$\tilde{\lambda}$	bulk thermal conductivity tensor or effective conductivity tensor		$[\mathrm{W\,m^{-1}\,K^{-1}}]$
δ	thermal diffusivity	$[\mathrm{m^2\,s^{-1}}]$	
μ	dynamic viscosity	[Pa s]	
ρ	density	$[\mathrm{kg\,m^{-3}}]$	
φ	porosity		

Subscripts, superscripts

0	reference condition
dw	downward
f	fluid
i	inner

627	*in*	inlet
628	*o*	outer
629	*out*	outlet
630	*s*	soil property
631	*up*	upward
632	*w*	water

Figures

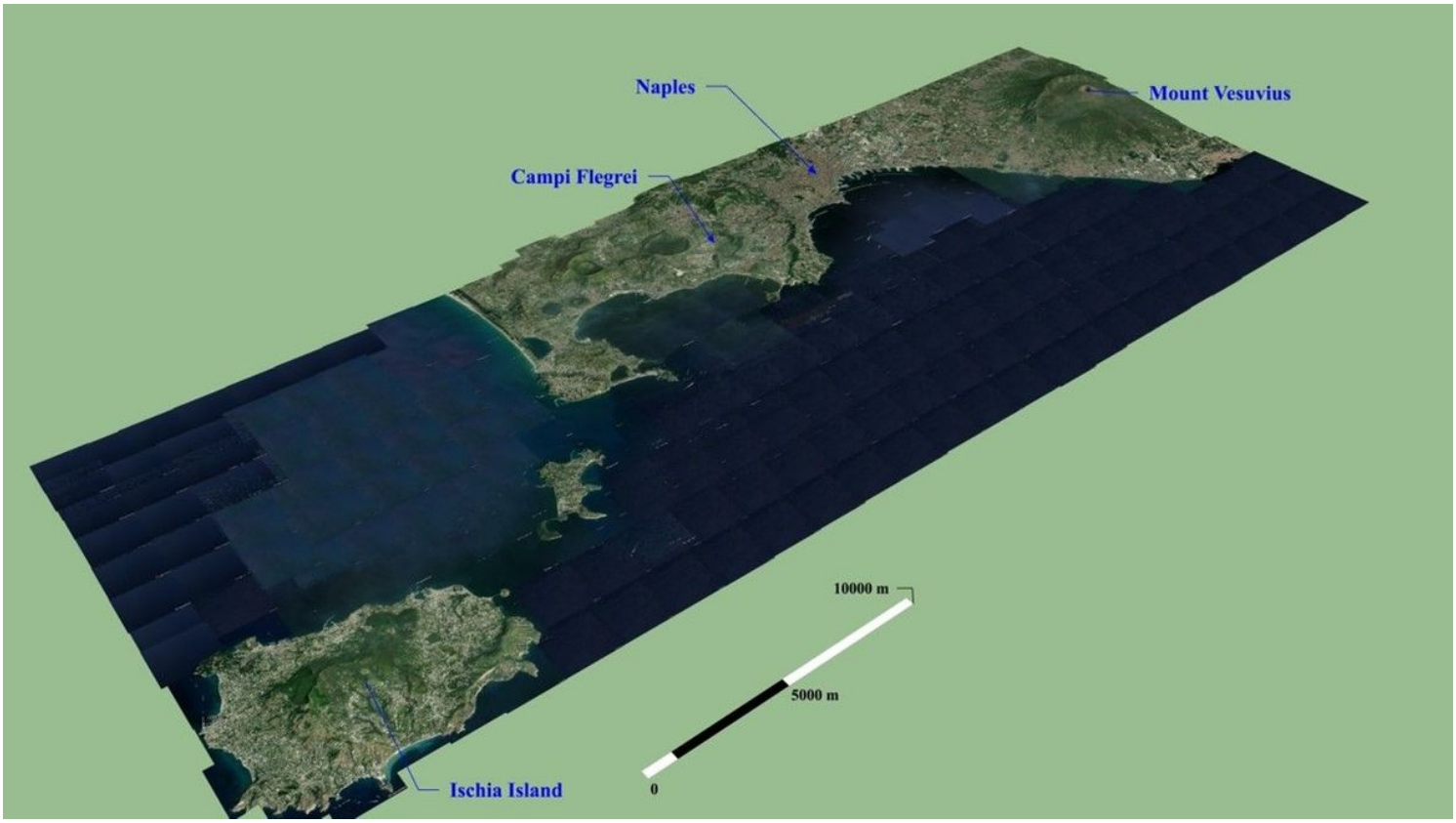

Figure 1

The Napolitan volcanoes district.

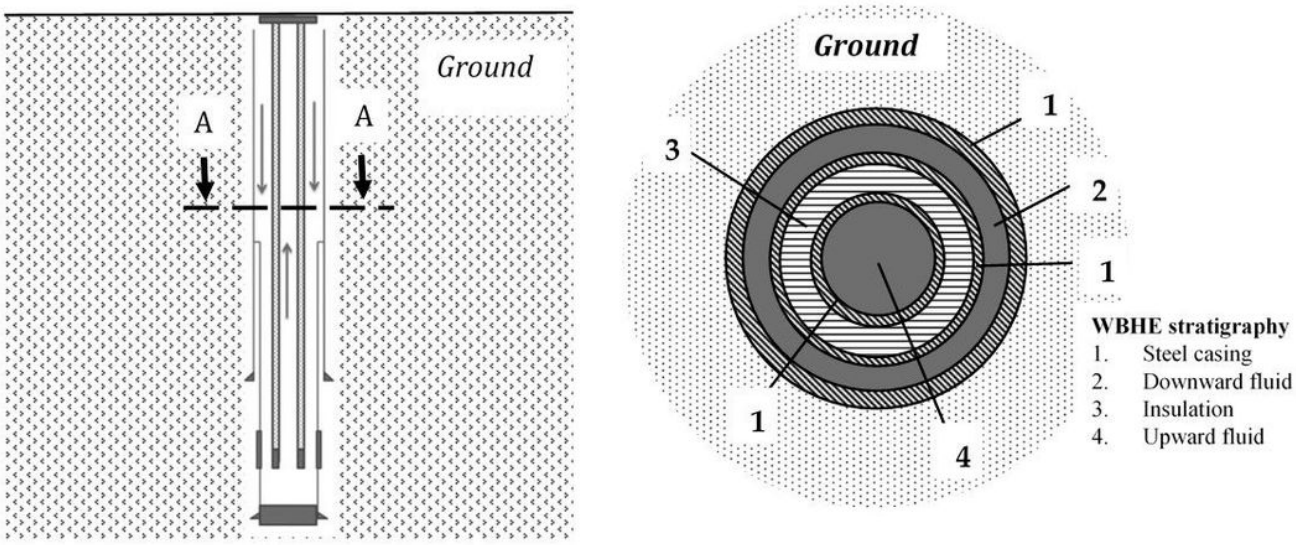

Figure 2

The coaxial heat exchanger.

Figure 3

CampiFlegrei caldera.

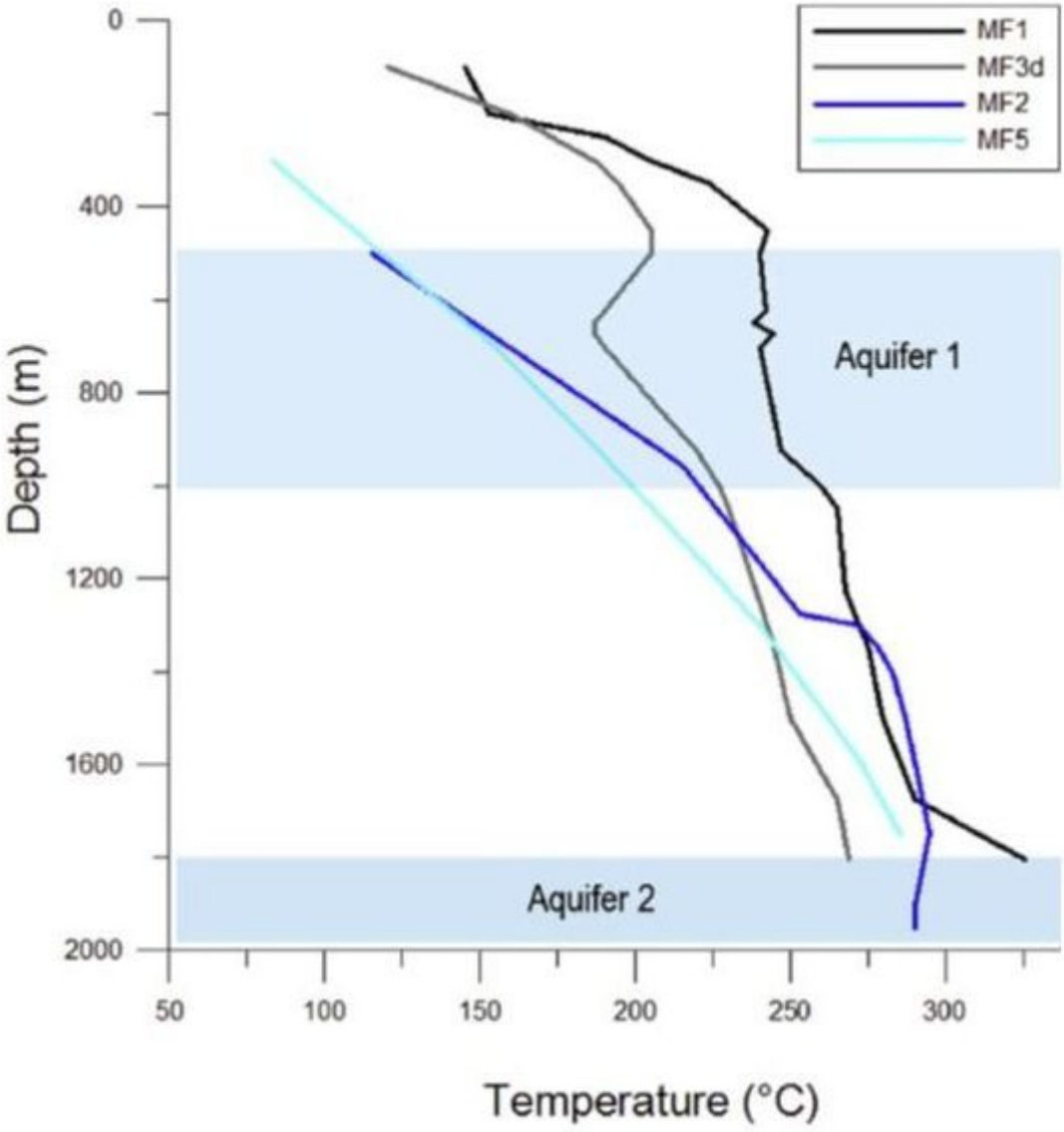

Figure 4

Temperature profiles with depth (Carlino et al. 2012).

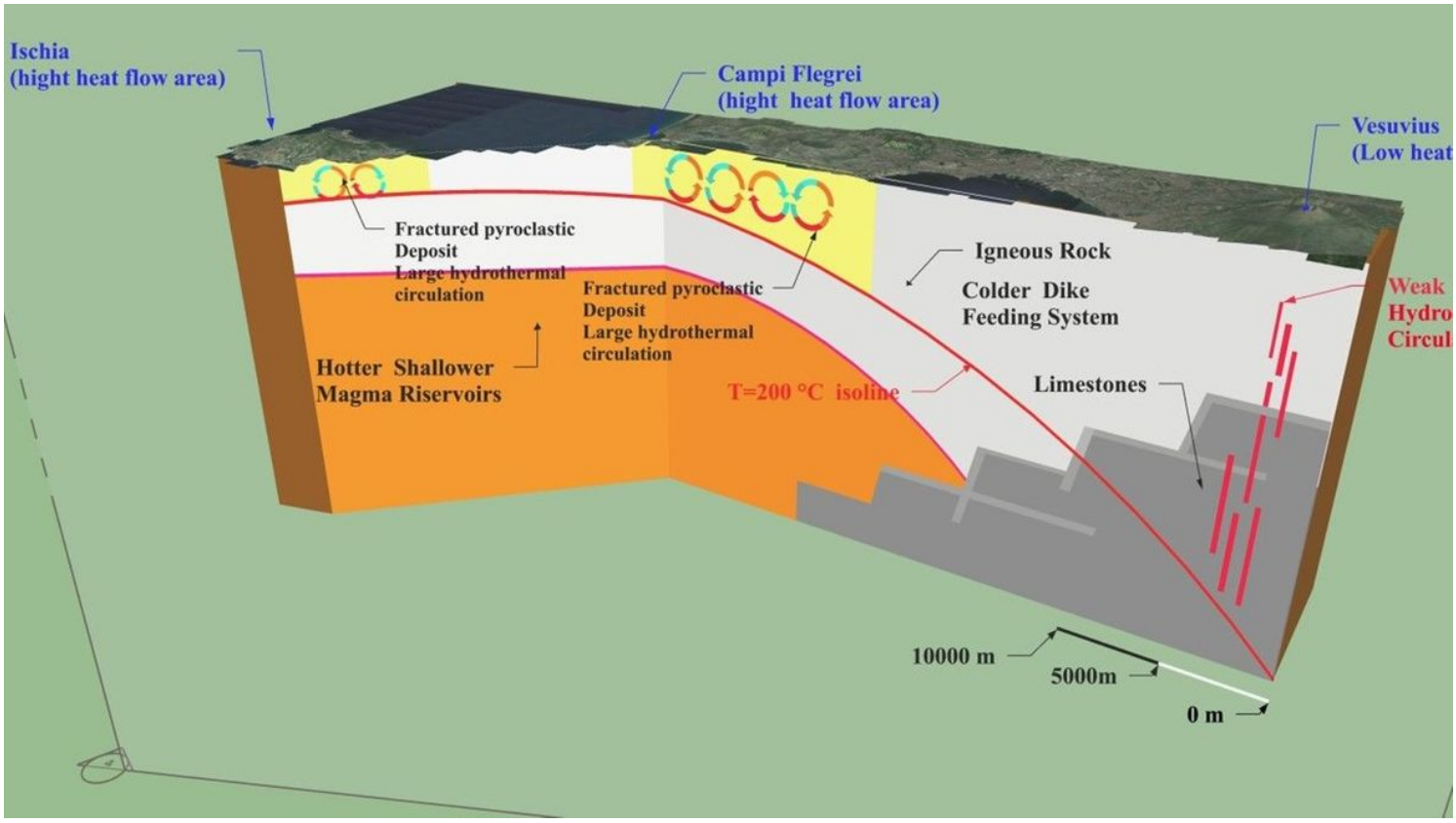

Figure 5

Sketch of the geothermal system under the Neapolitan volcanoes district.

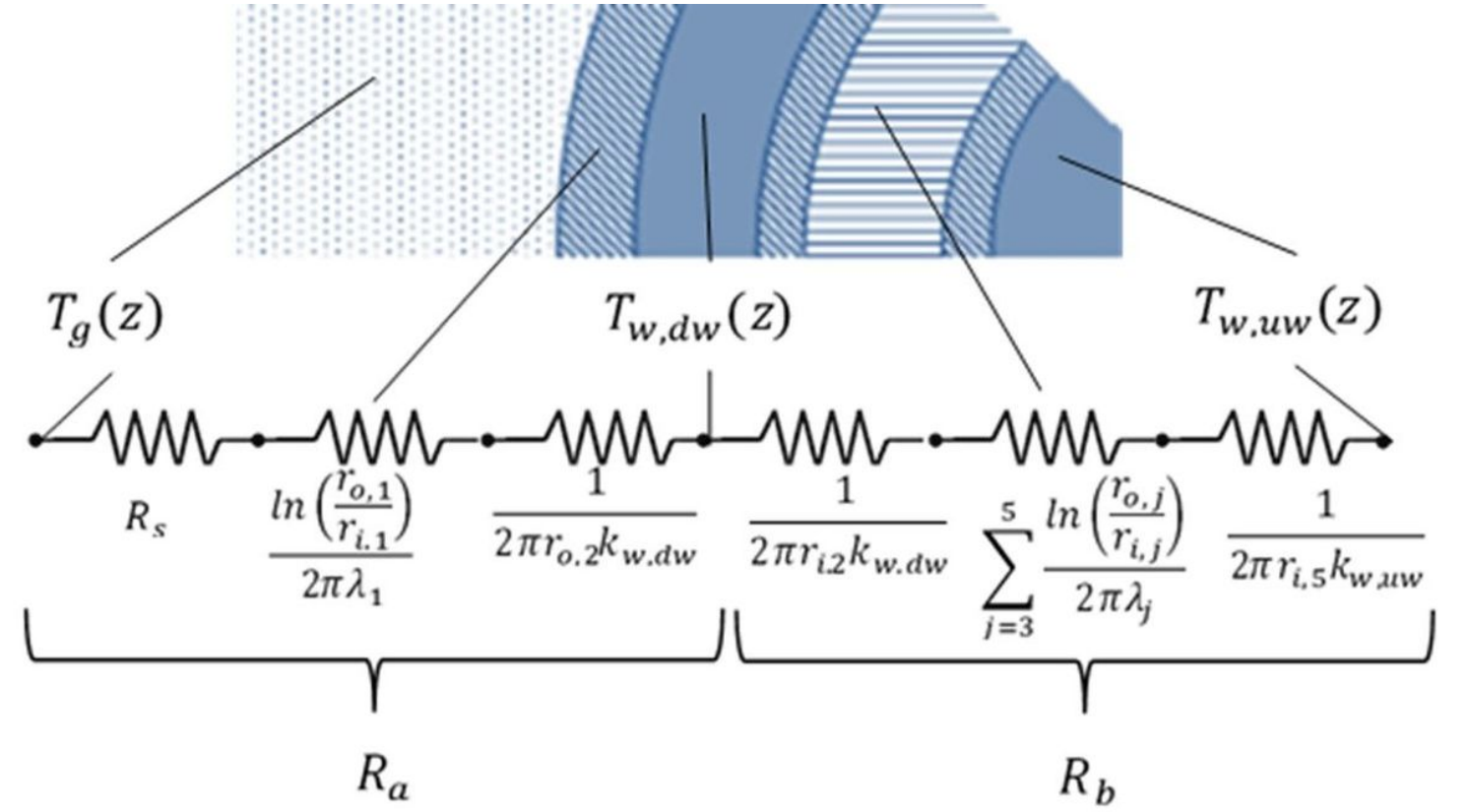

Figure 6

Thermal resistances of the deep borehole heat exchanger.

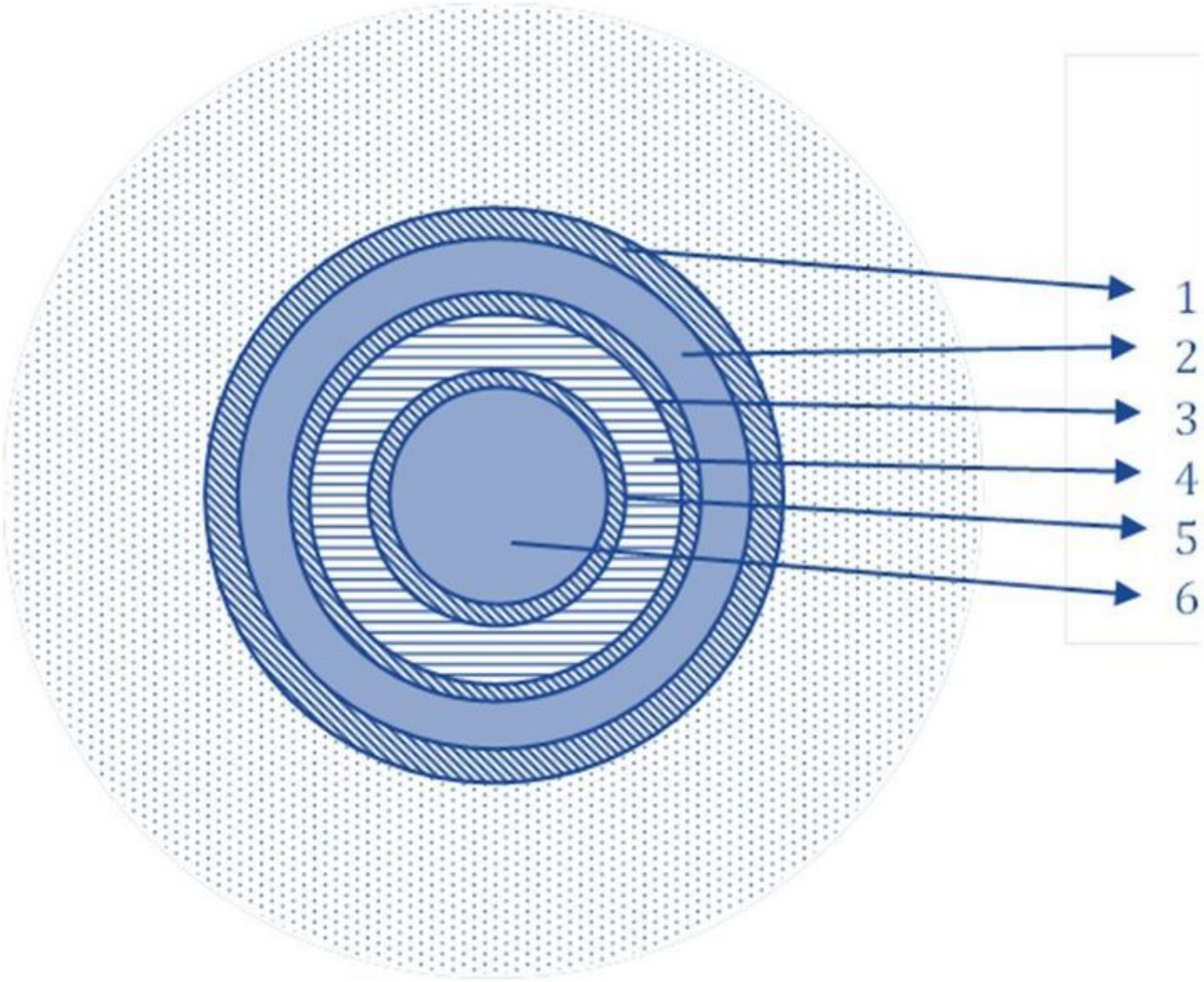

Figure 7

Deep borehole heat exchanger: axial view and materials.

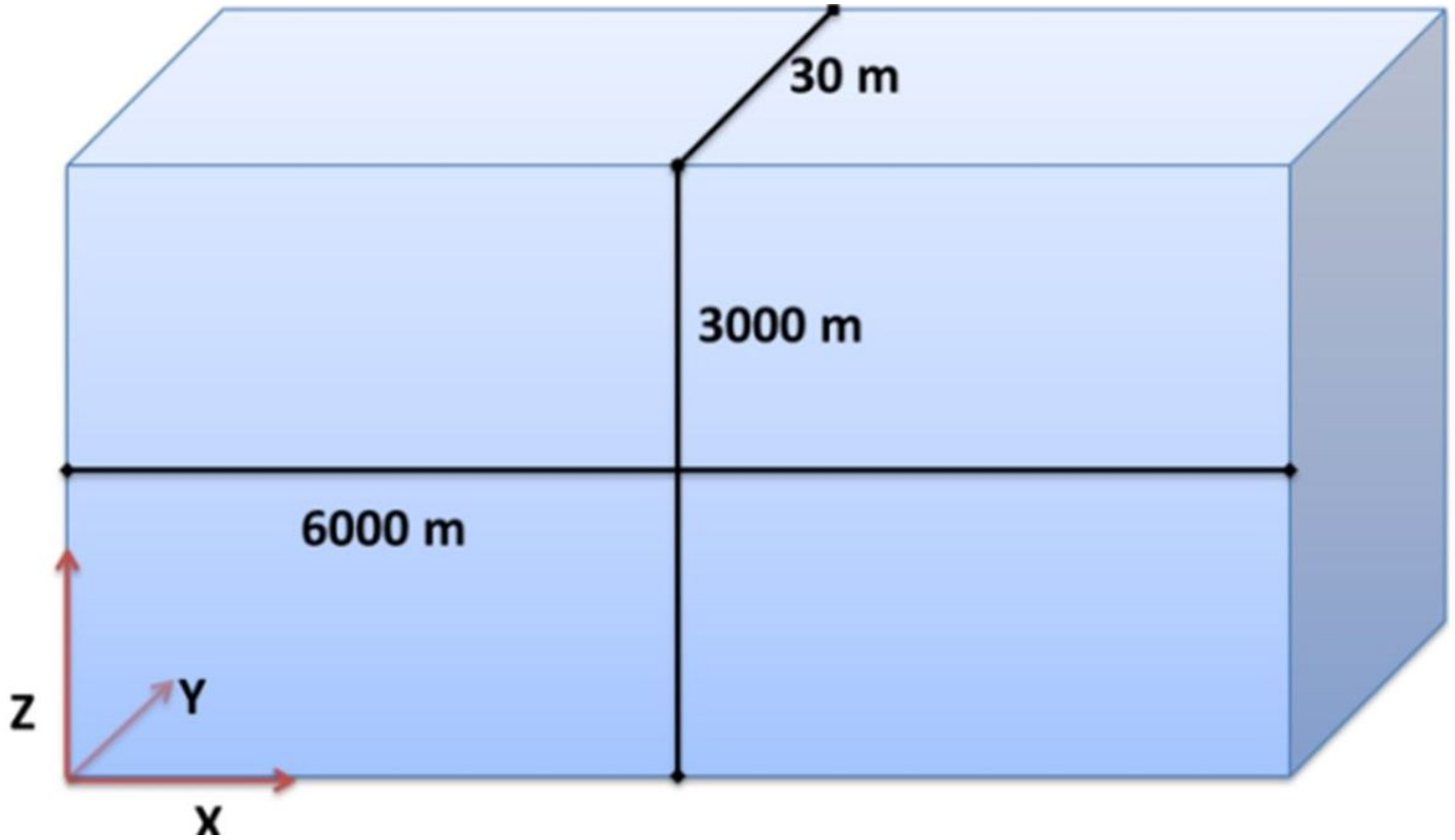

Figure 8

CampiFlegrei domain.

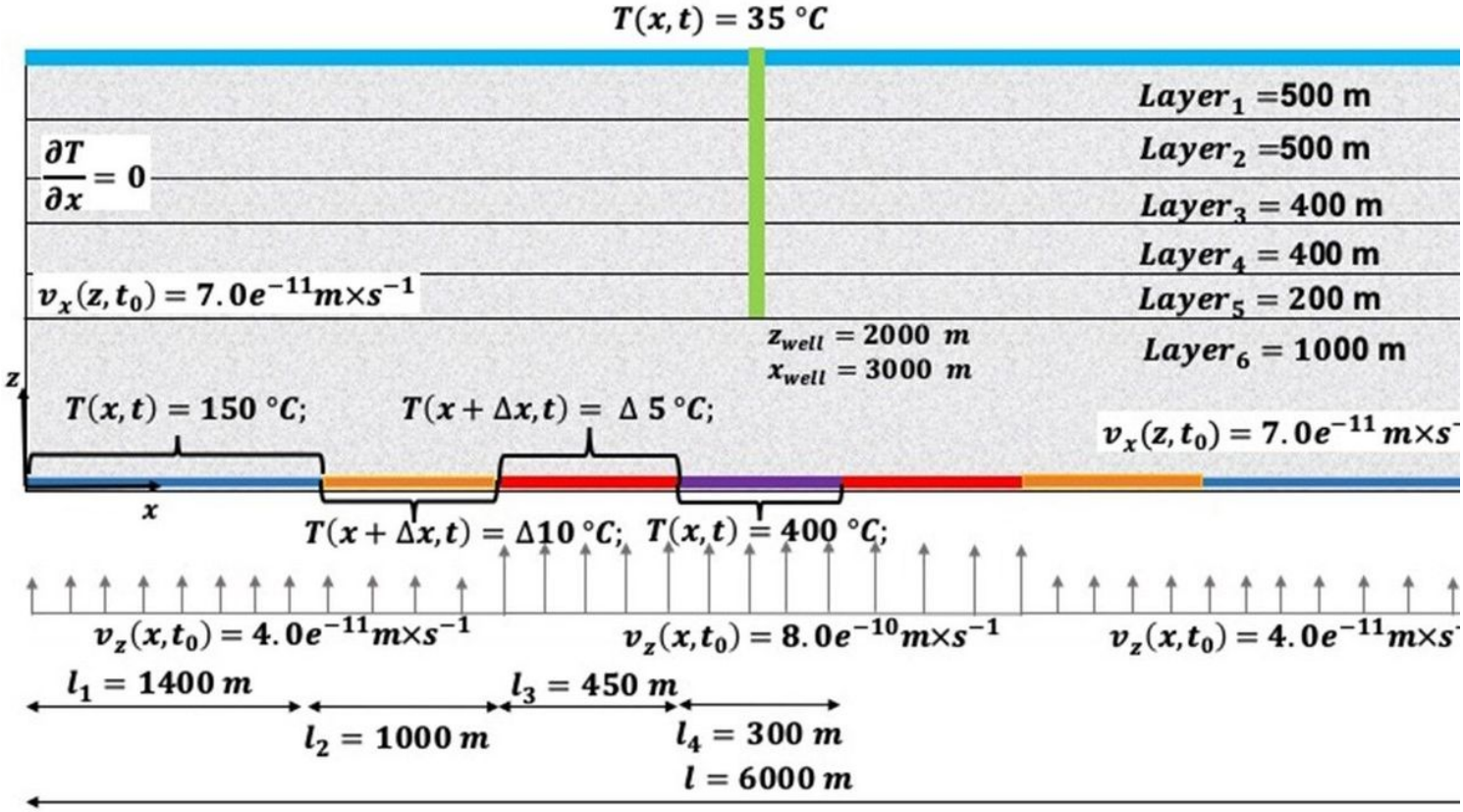

Figure 9

Boundary conditions imposed in SHEMAT model of CampiFlegrei.

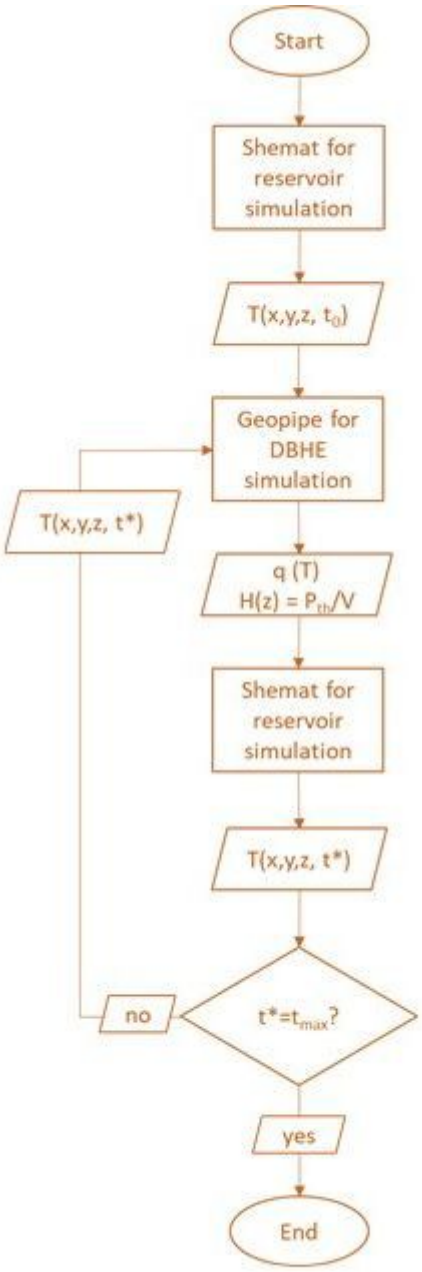

Figure 10 (a) – Method A

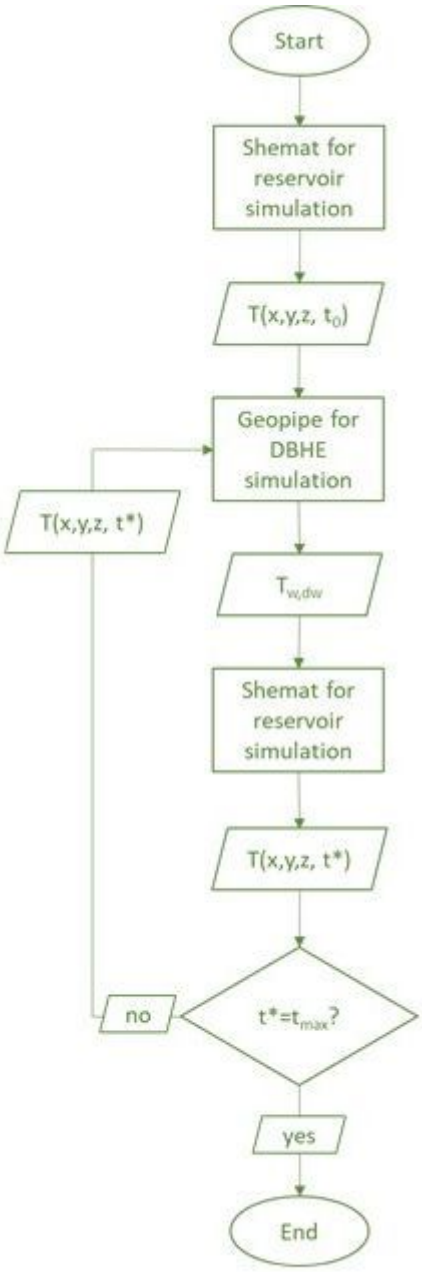

Figure 10 (b) – Method B

Figure 10

Figure 10 (a) – Method A Figure 10 (b) – Method B Figure 10: Workflow of the two models coupling.

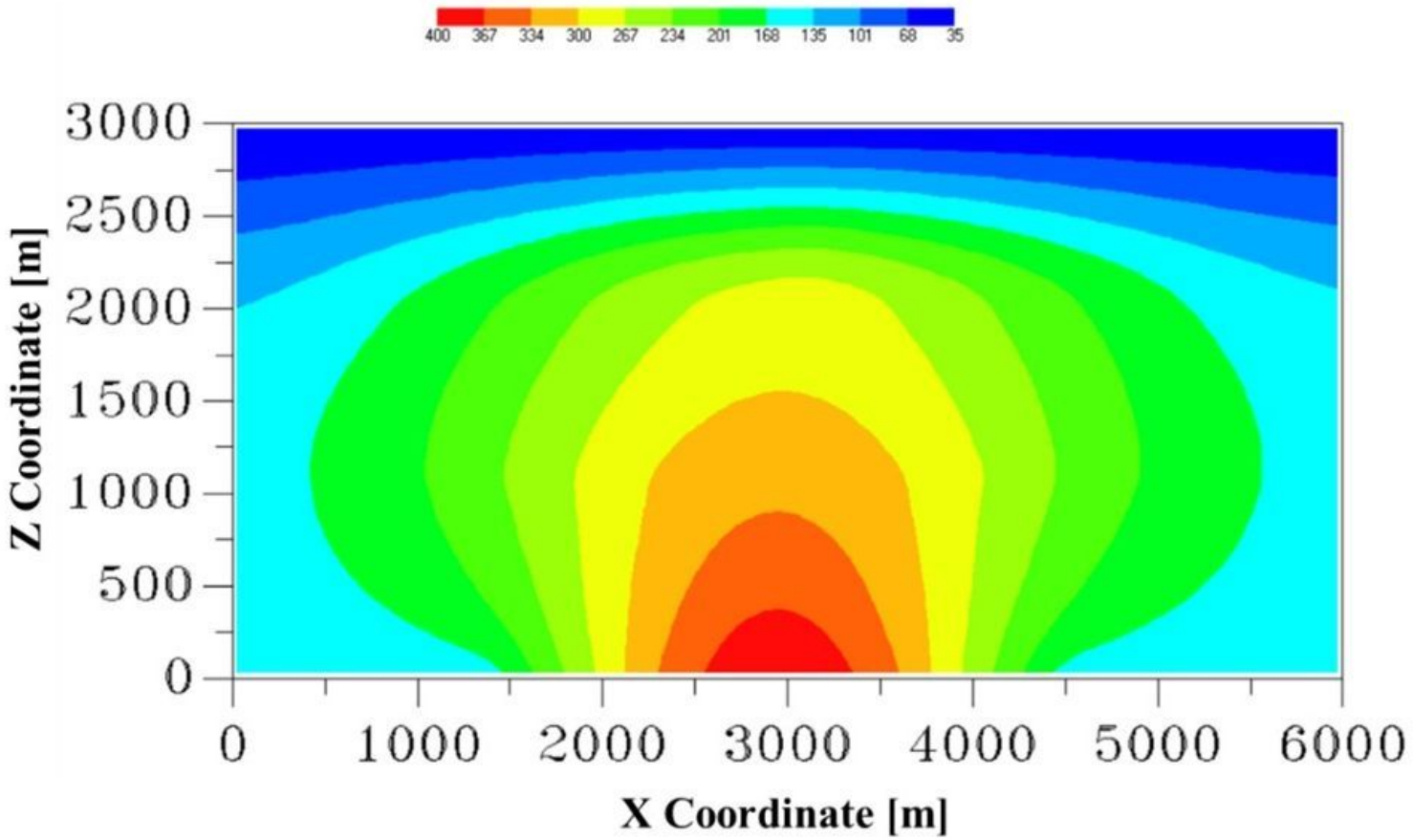

Figure 11

Initial temperature pattern.

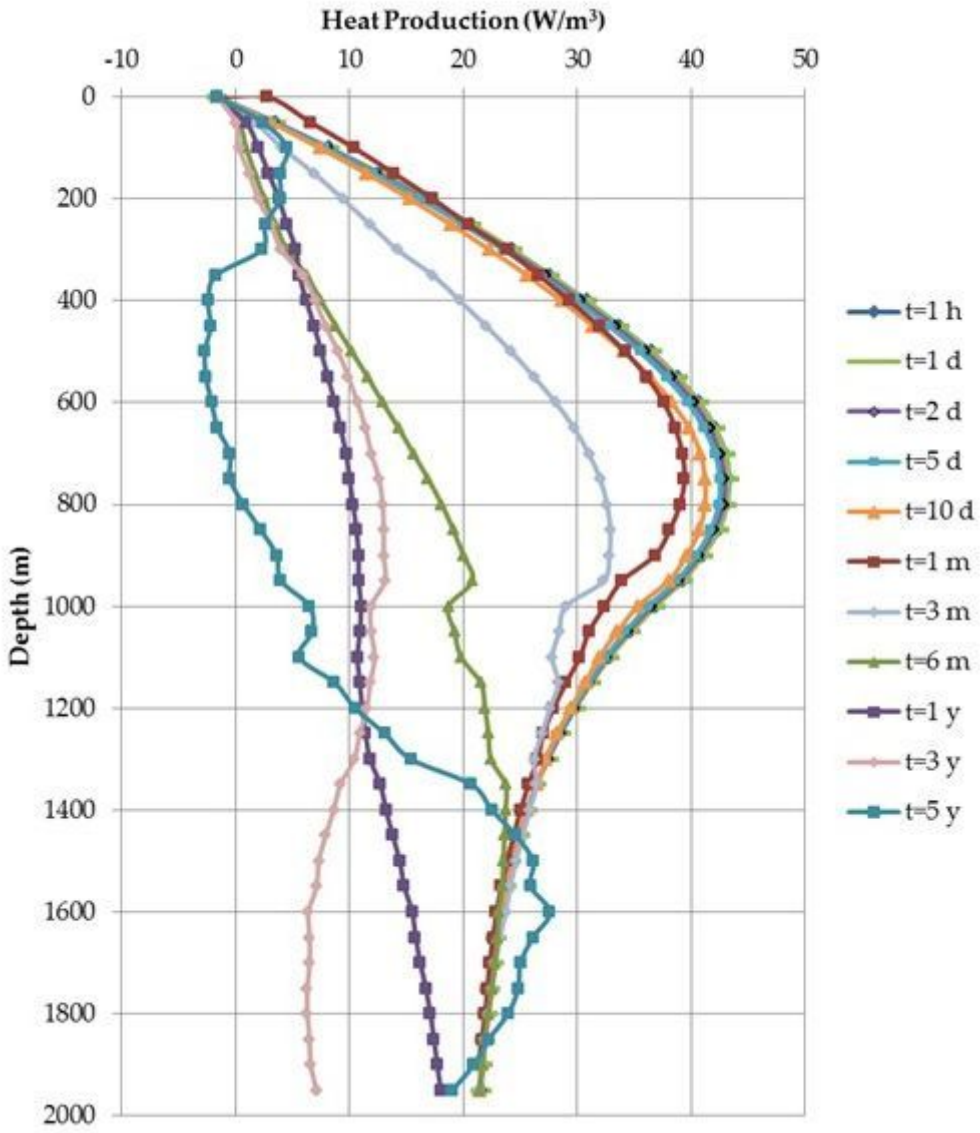

Figure 12

Heat extracted in time vs depth (SHEMAT – GEOPIPE model); fixed flow rate scenario.

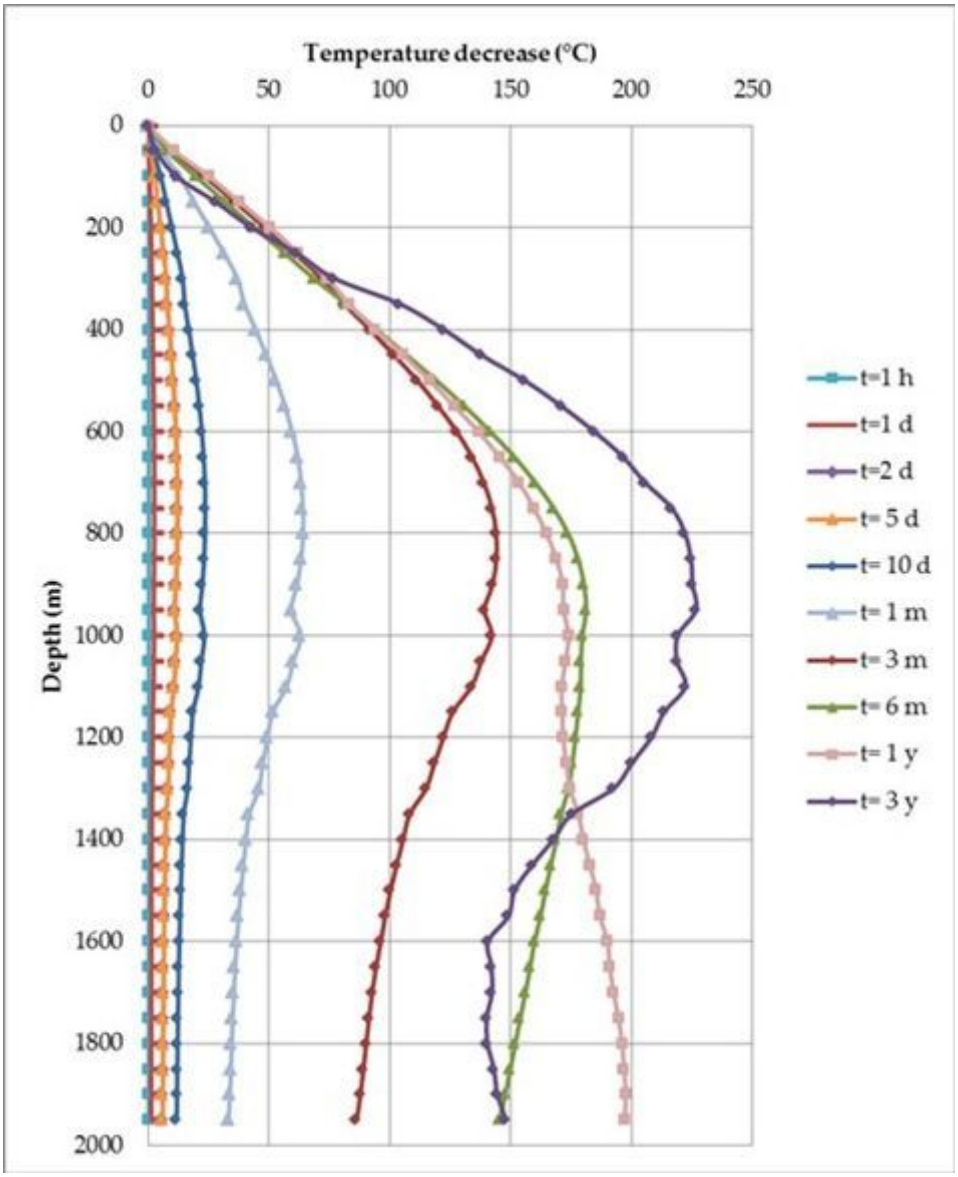

Figure 13

Decrease of the ground temperature in contact with the DBHE (SHEMAT – GEOPIPE model; fixed flow rate scenario.

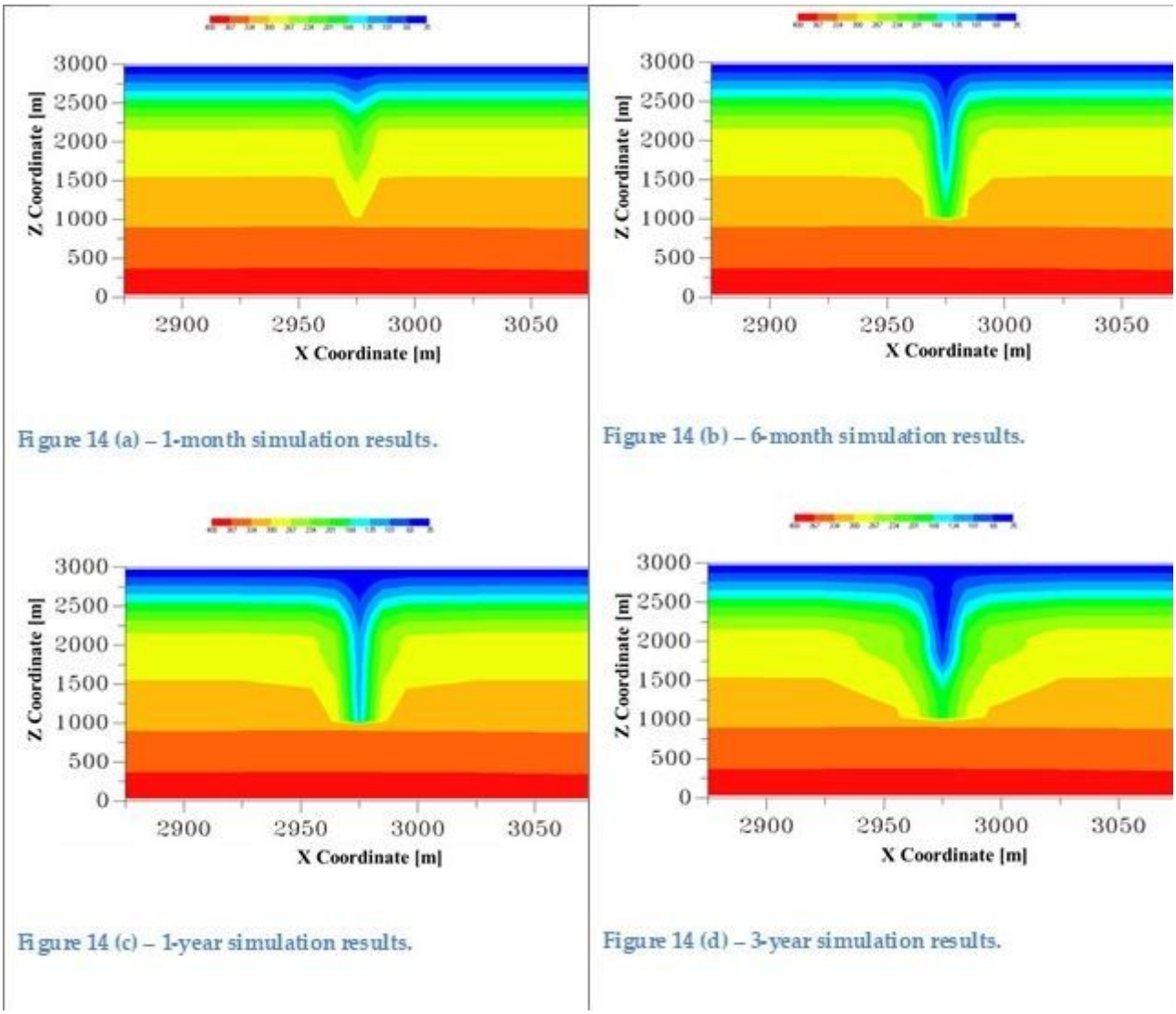

Figure 14 (a) – 1-month simulation results.

Figure 14 (b) – 6-month simulation results.

Figure 14 (c) – 1-year simulation results.

Figure 14 (d) – 3-year simulation results.

Figure 14

Figure 14 (a) – 1-month simulation results. Figure 14 (b) – 6-month simulation results. Figure 14 (c) – 1-year simulation results. Figure 14 (d) – 3-year simulation results. Figure 14- Thermal disturbance variation; fixed flow rate scenario.

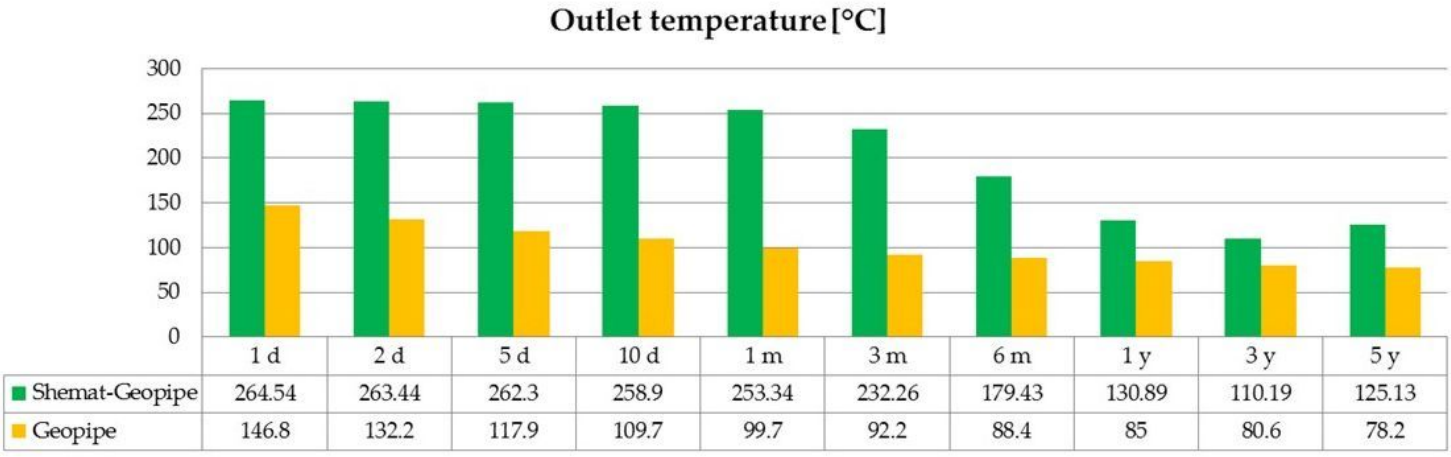

	1 d	2 d	5 d	10 d	1 m	3 m	6 m	1 y	3 y	5 y
Shemat-Geopipe	264.54	263.44	262.3	258.9	253.34	232.26	179.43	130.89	110.19	125.13
Geopipe	146.8	132.2	117.9	109.7	99.7	92.2	88.4	85	80.6	78.2

Figure 15

Decrease of water temperature extracted by a zero-mass extraction device; fixed flow rate scenario.

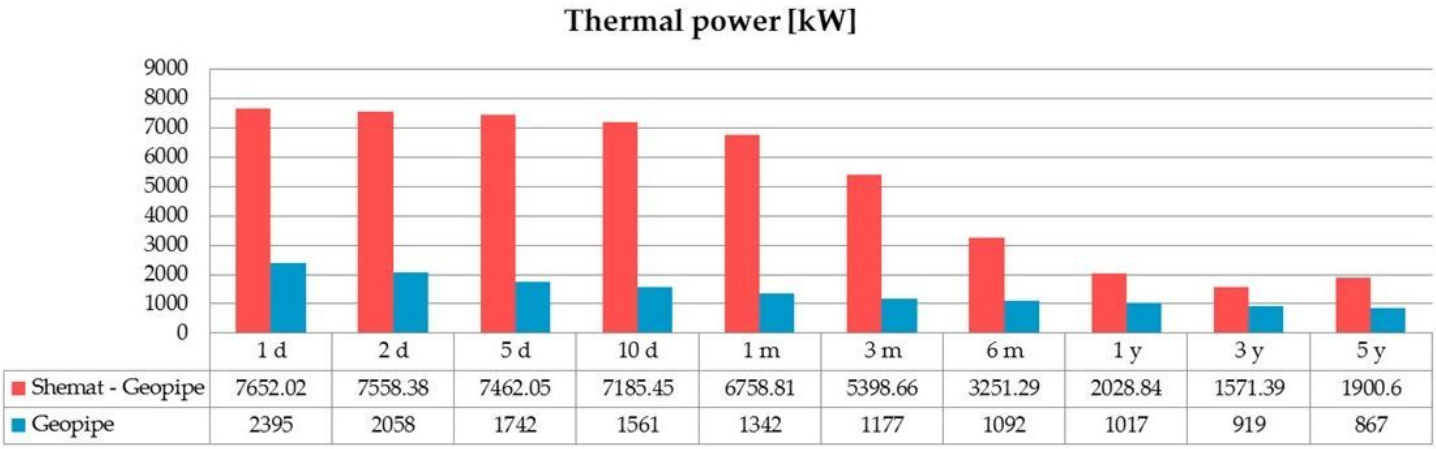

	1 d	2 d	5 d	10 d	1 m	3 m	6 m	1 y	3 y	5 y
Shemat - Geopipe	7652.02	7558.38	7462.05	7185.45	6758.81	5398.66	3251.29	2028.84	1571.39	1900.6
Geopipe	2395	2058	1742	1561	1342	1177	1092	1017	919	867

Figure 16

Sustainability in time of a zero-mass extraction plant; fixed flow rate scenario.

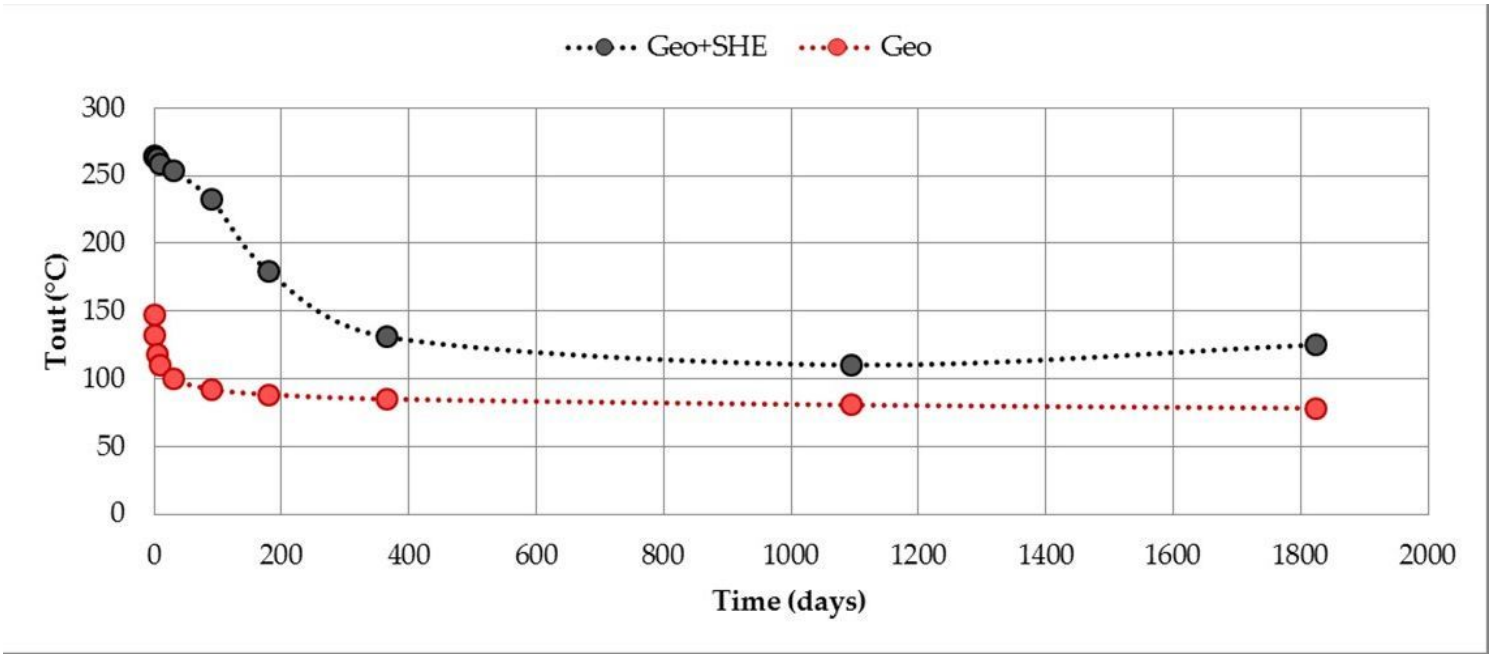

Figure 17

Thermal decline in time; fixed flow rate scenario.

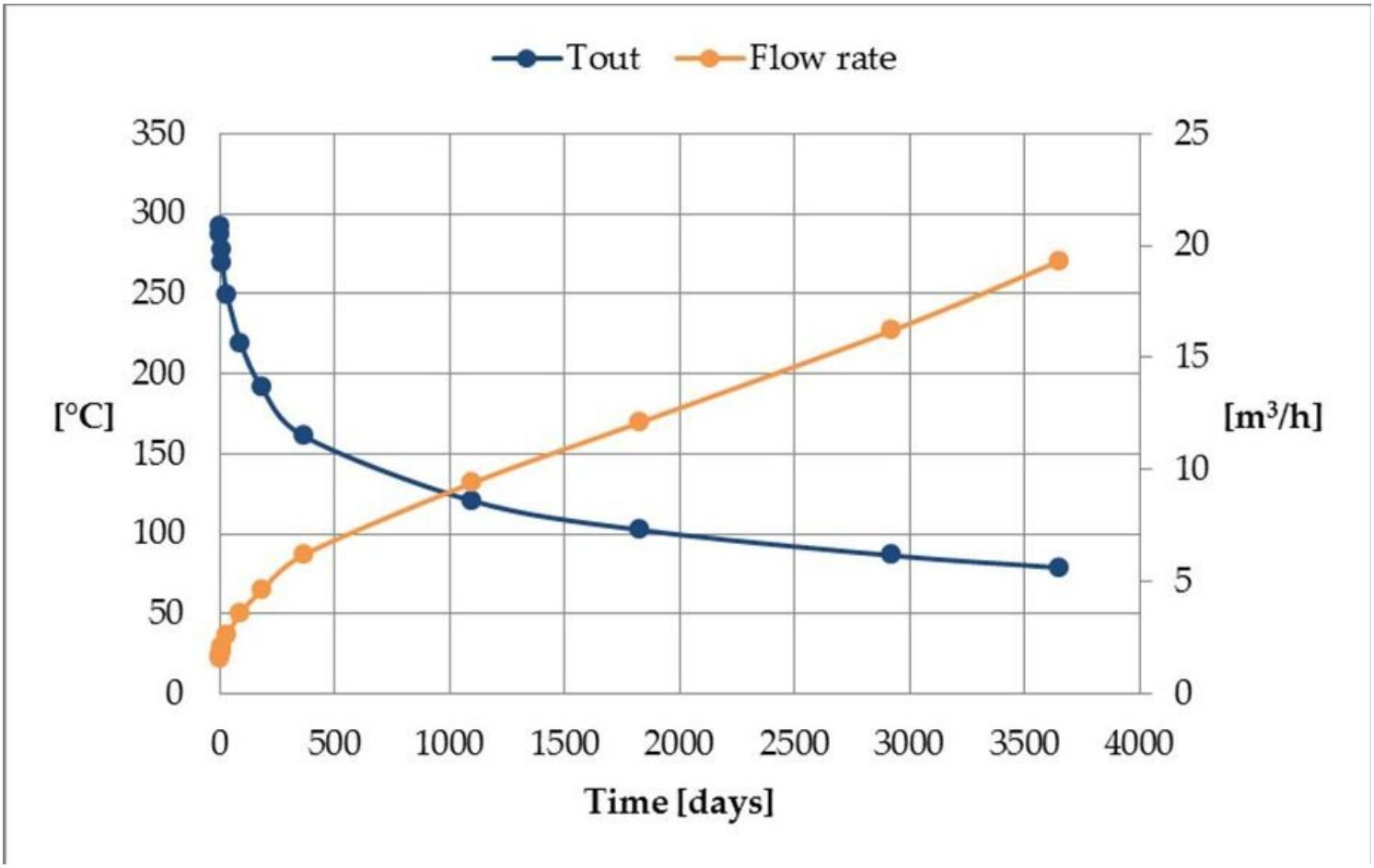

Figure 18

Variation of flow rate and outlet temperature for a DBHE operating at a fixed thermal power of 850 kW; Geopipe results.

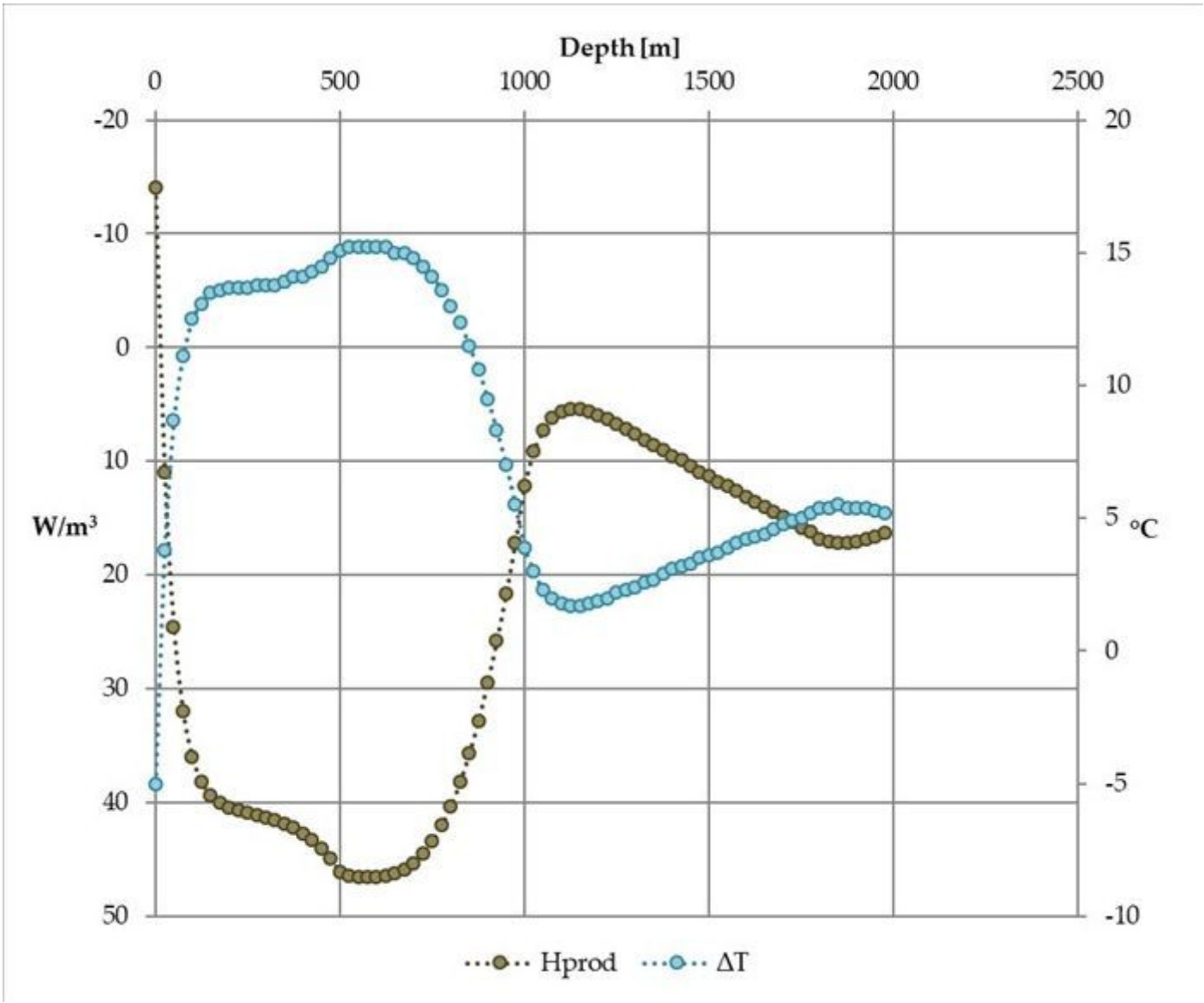

Figure 19

Heat production along with depth at a fixed thermal power of 850 kW.

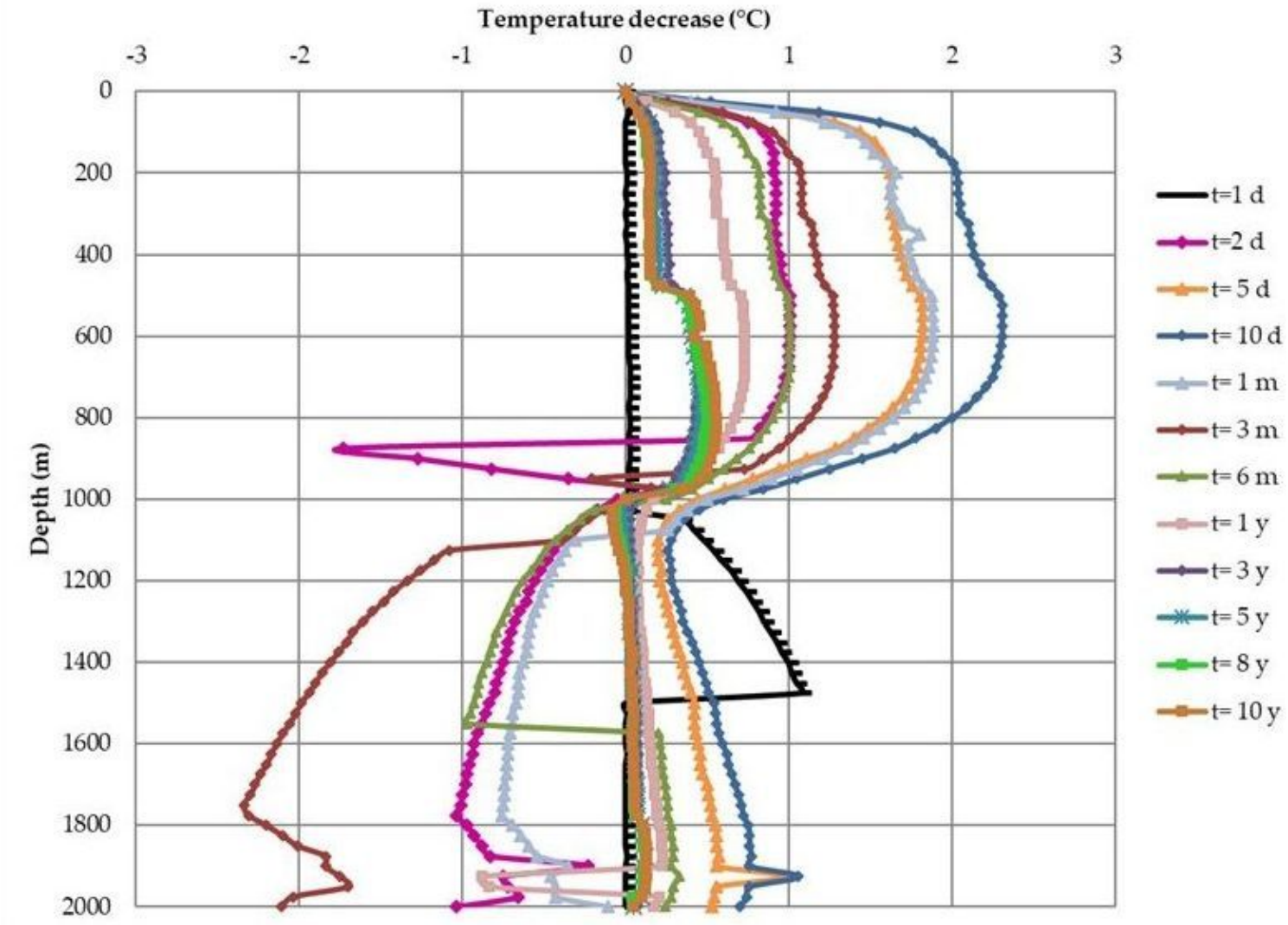

Figure 20

Decrease of the ground temperature in contact with the DBHE (SHEMAT – GEOPIPE model; fixed thermal power scenario.

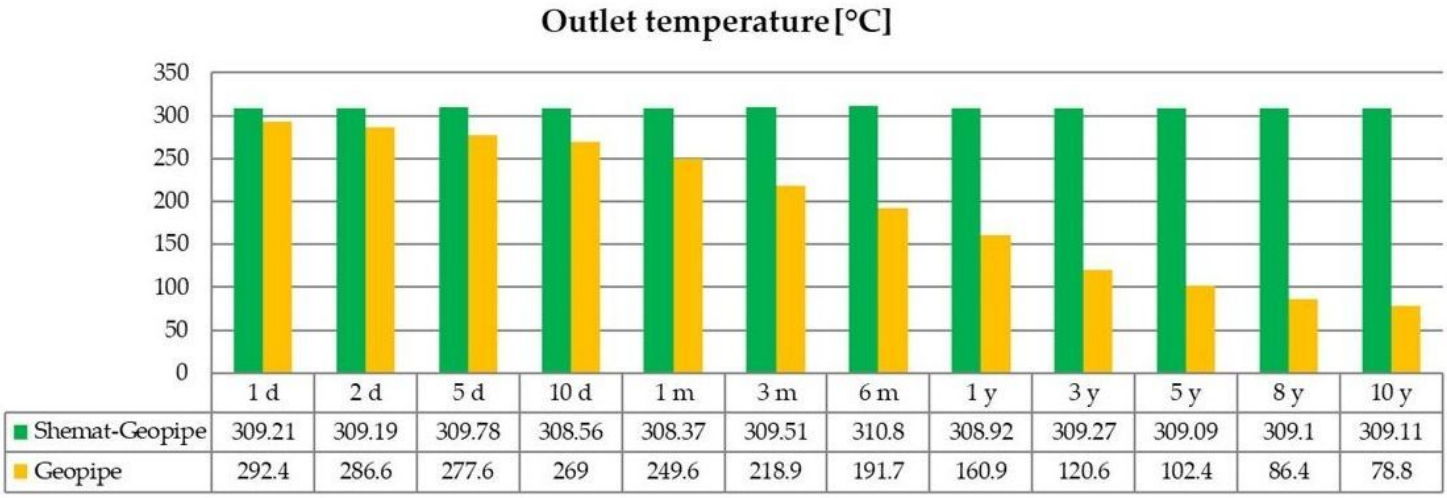

	1 d	2 d	5 d	10 d	1 m	3 m	6 m	1 y	3 y	5 y	8 y	10 y
Shemat-Geopipe	309.21	309.19	309.78	308.56	308.37	309.51	310.8	308.92	309.27	309.09	309.1	309.11
Geopipe	292.4	286.6	277.6	269	249.6	218.9	191.7	160.9	120.6	102.4	86.4	78.8

Figure 21

Decrease of water temperature extracted by a zero-mass extraction device; fixed thermal power scenario.

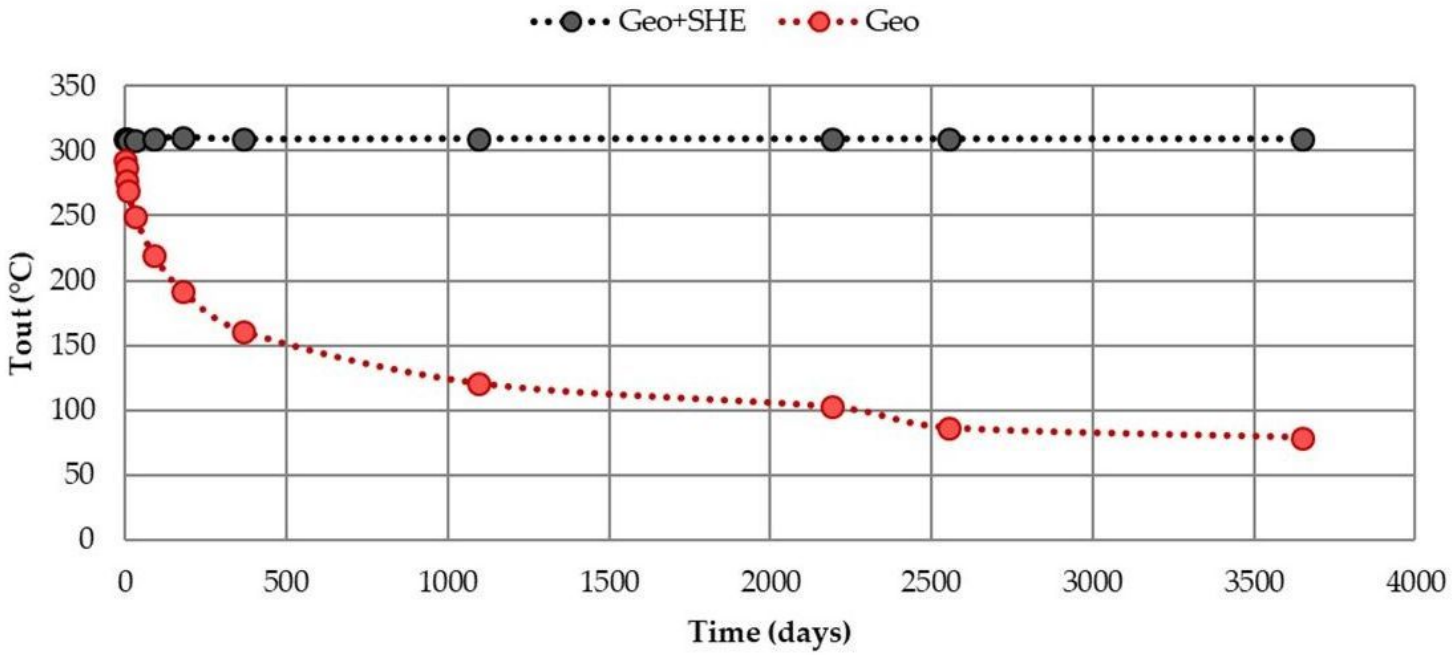

Figure 22

Thermal decline in time; fixed thermal power scenario.